UNCLASSIFIED

AD NUMBER
AD483748
LIMITATION CHANGES
TO: **Approved for public release; distribution is unlimited.**
FROM: **Distribution authorized to U.S. Gov't. agencies and their contractors; Administrative/Operational Use; JUN 1966. Other requests shall be referred to Arnold Engineering Developmental Center, Arnold AFB, TN.**
AUTHORITY
AEDC ltr 29 Jan 1996

THIS PAGE IS UNCLASSIFIED

AEDC-TR-66-73

AEDC/PA 96-026

H Ball

TURBULENT CAVITY FLOW INVESTIGATION AT MACH NUMBERS 4 AND 8

J. P. Rhudy and J. D. Magnan, Jr.
ARO, Inc.

June 1966

VON KÁRMÁN GAS DYNAMICS FACILITY

ARNOLD ENGINEERING DEVELOPMENT CENTER

AIR FORCE SYSTEMS COMMAND

ARNOLD AIR FORCE STATION, TENNESSEE

NOTICES

TURBULENT CAVITY FLOW INVESTIGATION AT MACH NUMBERS 4 AND 8

J. P. Rhudy and J. D. Magnan, Jr.
ARO, Inc.

FOREWORD

The work reported herein was done at the request of Headquarters, Arnold Engineering Development Center (AEDC), Air Force Systems Command (AFSC), under Program Element 62405334, Project 8953, Task 895303.

The results of research presented were obtained by ARO, Inc. (a subsidiary of Sverdrup & Parcel and Associates, Inc.), contract operator of AEDC, AFSC, Arnold Air Force Station, Tennessee, under Contract AF 40(600)-1200. The research was conducted at intervals during the period December 1962 to November 1963 under ARO Project No. VT2081, and the manuscript was submitted for publication on March 14, 1966.

Publication of this report does not constitute Air Force approval of the report's findings or conclusions. It is published only for the exchange and stimulation of ideas.

Larry R. Walter
1/Lt, USAF
Gas Dynamics Division
DCS/Research

Donald R. Eastman, Jr.
DCS/Research

ABSTRACT

An experimental investigation of turbulent flow over a cavity in an aerodynamic surface has been conducted. The test was carried out at nominal Mach numbers of 4 and 8, with Reynolds numbers based on free-stream conditions and length of body ahead of the cavity of 8.0×10^6 and 11.0×10^6, respectively. Two conditions of wall-to-free-stream stagnation temperature ratio, 0.4 and 0.8, were investigated at $M_\infty = 8.09$, whereas at $M_\infty = 3.99$, the temperature ratio was 0.75. For all tests, the ratio of initial boundary-layer thickness to cavity depth was approximately 0.2. Measurements were made of surface pressure and temperature, and flow field surveys of pitot and static pressures and total temperature were performed. The test results showed that the recirculating fluid temperature was not less than 0.7 times the free-stream stagnation temperature despite decrease of the wall temperature to 0.4 the free-stream value. A satisfactory correlation was obtained between the experimental velocities and the error function profile of Goertler, and the distribution of total temperature across the mixing layer was adequately described by Crocco's linear relation of total temperature and velocity. A value of the mixing zone similarity parameter near 12 was found regardless of Mach number or wall-to-free-stream stagnation temperature ratio.

CONTENTS

ILLUSTRATIONS

TABLES

NOMENCLATURE

a	Constant in velocity-temperature relation (Appendix I)
b	Constant in velocity-temperature relation (Appendix I); also, width of mixing layer (Appendix III and Fig. 11)
C	Constant in universal velocity profile integral (Appendix II)
c	Constant expressing linear growth of mixing layer width b (Appendix III) with distance from start of mixing
F	Modified stream function in error function profile differential equation (Appendix III)
K	Constant in relation between mixing length ℓ and y distance from wall (Appendix II); also K_1, constant in turbulent shear stress equation (Appendix III)
ℓ	Distance parallel to axis of model, in.; $\ell = 0$ at upstream edge of cavity, ℓ positive downstream; also, mixing length in Prandtl's hypothesis (Appendix II)
M	Mach number
O	Origin of mixing layer profiles (Appendix III and Fig. 11)
p	Pressure, psia
R	Radial distance from centerline of model, in.
Re	Unit Reynolds number, 1/ft
T	Temperature, °R
u	Streamwise velocity component, ft/sec
u_τ	Friction velocity $u_\tau = \sqrt{\frac{\tau_w}{\rho}}$
v	Velocity component, normal to streamwise velocity, ft/sec
x	Distance from origin of mixing layer in flow direction, in.; $x = o$ at origin of mixing layer (Appendix III and Fig. 11)
y	Distance normal to mixing layer, in.; $y = 0$ at $\frac{u}{u_\delta} = 0.5$ point in mixing layer velocity profile (Appendix III and Fig. 11); also, distance normal to body surface (Appendix II)
ϵ	Turbulent eddy kinematic viscosity, ft^2/sec
θ	Angle between rays of constant $\frac{u}{u_g}$ in mixing zone, radians (Fig. 11)

μ Laminar molecular viscosity, lb_f-sec/ft^2

ν Laminar molecular kinematic viscosity, ft^2/sec

ρ Density of fluid, lb_f-sec^2/ft^4

σ Mixing zone similarity parameter, dimensionless

SUBSCRIPTS

o Stagnation condition, with x, referring to distance from upstream edge of cavity to origin of mixing layer profiles

w Wall condition, thermal properties evaluated at wall temperature

δ Conditions at high velocity edge of boundary or mixing layer

∞ Free-stream condition in wind tunnel

SUPERSCRIPT

′ Pitot pressure

SECTION I
INTRODUCTION

A separated flow may be produced by either imposing a pressure rise on an established boundary layer, as by deflecting a control surface, or by terminating the surface on which the boundary layer has developed, as occurs at the base of bodies and at the upstream edge of surface cavities. Such flows are of considerable interest to flight vehicle designers because of their association with problems of control effectiveness, base drag, and base heating of missiles. The separated flow over a cavity is of interest in those cases where recesses are to be found in the aerodynamic surface of flight vehicles.

In response to the need for understanding of separated flows, several authors have presented work covering various aspects of the problem. Crocco and Lees (Ref. 1) published a very general integral approach to the calculation of laminar or turbulent separated flow fields which has been applied by Glick (Ref. 2) to the case of laminar boundary-layer shock wave interaction. Chapman (Ref. 3) solved the boundary-layer equations for laminar flow over a cavity, and Larson (Ref. 4) performed wind tunnel tests in the supersonic speed range using Chapman's mathematical model as a guide to the design of the experiment. The work of Korst and Chow (Ref. 5) is particularly interesting in that it derives one fixed profile form each for velocity and total temperature of a fully developed turbulent separated flow and relates these profiles to the flow geometry of the actual problem through a set of integral relations. Larson and coworkers (Ref. 6) published the results of detailed studies of a turbulent base separation at a supersonic Mach number. None of the above theoretical approaches (Refs. 1, 3, and 5) in its most general form, is sufficient in itself to calculate the turbulent separated flow over a cavity or at the base of a vehicle. Additional empirical information must be provided which can be verified only by experiments such as those of Refs. 4 and 6. For example, in the theoretical work of Chapman, in the absence of experimental data on cavity flow total temperature distributions, the assumption was made that the temperature of the recirculating fluid under the separated boundary layer was equal to the body wall temperature. The experimental work of Larson (Ref. 4) supplied data which indicated the recirculating fluid temperature remained closer to the free-stream total temperature than to the wall temperature, and Chapman's assumption could be amended. Korst and Chow (Ref. 5) derive the velocity profile of the separated boundary layer to be the error function profile of Goertler and assume that the temperature-velocity relation of Crocco is valid. A similarity parameter, σ, appears in the Korst and Chow theory, and the total temperature ratio across the mixing layer must be determined and verified by experiment.

The purpose of the present tests was to support such theoretical analysis with detailed experimental turbulent cavity flow field data at a hypersonic Mach number. The experiment was designed to produce data with the simplest initial and boundary conditions possible, to correspond with the assumptions usually made in mathematical analysis. An internally air-cooled, 20-cal, tangent ogive cylinder model was made, with the cavity, formed by a reduction in cylinder diameter, located well aft in a region of uniform parallel flow. The model static pressure and wall temperature were held constant for some distance upstream on the forebody. The large size of the 40-in. supersonic tunnel (Gas Dynamic Wind Tunnel, Supersonic (A)) and the 50-in. Mach 8 tunnel (Gas Dynamic Wind Tunnel, Hypersonic (B)) of the von Kármán Gas Dynamics Facility (VKF) admitted a model long enough to produce a naturally turbulent boundary layer at the upstream edge of the cavity, and the continuous flow in these wind tunnels allowed detailed flow surveys to be made for various steady experimental conditions.

The tests were performed at Mach numbers of 3.99 and 8.09, at free-stream unit Reynolds numbers of 2.4 and 3.3 million/ft, respectively. At Mach 8.09, data were obtained for two values, 0.4 and 0.8, of wall-to-free-stream stagnation temperature.

SECTION II
APPARATUS

2.1 MODEL

The model (Fig. 1) was a 20-cal tangent ogive cylinder of 58.5-in. overall length and 5.5-in. diameter. The cavity section began 40.5 in. aft on the model and continued for 6 in. at a reduced diameter of 2.0 in., providing a cavity of 1.75-in. radial depth. Air cooling was accomplished by double-wall construction of the model, allowing for a coolant passage between the inner liner and the model wall itself. The material was stainless steel.

The model forebody and cavity were instrumented both for static pressure measurement, using standard pressure orifices, and for steady-state surface temperature measurement.

For flow visualization studies, the model was fitted with a flow splitter plate, and motion-picture sequences of oil flow in the cavity were taken. The plate was not present except for this part of the test.

2.2 WIND TUNNELS

Tunnels A and B (Fig. 2) were used for this experiment. Tunnel A is a variable Mach number, flexible nozzle, supersonic tunnel with a 40-in. square test section. Tunnel B is a contoured axisymmetric tunnel with a Mach number, at 800-psia stagnation pressure, of 8.09, and a test section 50 in. in diameter. Both wind tunnels are capable of continuous operation using supply air from the VKF compressor plant (Ref. 7).

2.3 FLOW SURVEY PROBES

The forebody boundary layer at $M_\infty = 3.99$ was measured with a 10-tube pitot rake, each tube of which was 0.032 in. in diameter. The flow field surveys at this Mach number were made with a 0.062-in.-diam pitot probe and a total temperature probe consisting of a thermocouple inside a single, vented, 0.093-in.-diam tube. At $M_\infty = 8.09$, the pitot and flow field static pressures were measured simultaneously with a two-tube probe (Fig. 3a), each tube of which was 0.032 in. in diameter. The total temperature was measured with a double-shielded, vented, 0.125-in.-diam thermocouple probe (Fig. 3b), which was paired with a large diameter pitot probe for monitoring purposes.

2.4 FLOW VISUALIZATION EQUIPMENT

The shadowgraph equipment used was a standard, divergent-ray, spark shadowgraph system. For the oil flow work, a low viscosity silicone oil, with red dye added, was injected onto the model surface and the tapered flow splitter plate through the model static pressure orifices.

SECTION III
PROCEDURE

3.1 TEST CONDITIONS

The wind tunnel stagnation pressure and temperature were measured at each test condition and were used, with wind tunnel calibration data, to determine free-stream Mach and Reynolds numbers and to calculate the free-stream static pressure and temperature. The average operating conditions of the present test are outlined below:

M_∞	p_{o_∞}, psia	T_{o_∞}, °R	p_∞, psia	T_∞, °R	Re_∞/ft
3.99	37	675	0.247	161	2.4×10^6
8.09	800	1345	0.076	95	3.3×10^6

3.2 PROCEDURE

Following the establishment of steady flow in the wind tunnels, the model cooling air supply was adjusted until the forebody thermocouples indicated the desired model wall temperature. Model surface pressures and temperatures were then recorded. Following this, the survey probe was located at the desired model station and moved radially outward until the uniform external flow was reached. For the surveys of the reverse flow along the cavity floor, the above procedure was followed with the survey probe pointing downstream with respect to the free-stream direction. Table I contains a summary of measurements made.

3.3 DATA REDUCTION

3.3.1 Forebody Velocity Profiles

The forebody survey pitot pressures were combined with the wall static pressure, assumed constant across the boundary layer, to calculate local Mach number. For $M_\infty = 8.09$, $\frac{T_w}{T_{o_\infty}} = 0.8$, measured total temperatures, extrapolated to the wall temperature, were used, with the local Mach number, to calculate velocity. In the absence of measured total temperature at $M_\infty = 3.99$ and 8.09, $\frac{T_w}{T_{o_\infty}} = 0.4$, Crocco's relation between velocity and total temperature (Appendix I), was used in an iterative procedure to determine the velocity.

To determine the skin friction term appearing in the universal velocity profile correlation (Appendix II), the calculated velocities nearest the wall were used to form the derivative $\frac{du}{dy}$ at the wall.

3.3.2 Cavity Flow Field Profiles

The variation of Mach number across the mixing layer at $M_\infty = 3.99$ was obtained using the measured pitot pressures and the surface static pressure measured on the cavity floor at the station being surveyed, assuming this pressure to be constant across the mixing layer. Experimental total temperatures were used with these Mach numbers to calculate velocity.

The pitot pressure, flow field static pressure, and total temperature used in the calculations of mixing layer velocity were all measured at $M_\infty = 8.09$ except for $\frac{T_w}{T_{o_\infty}} = 0.4$, $\ell = 1.5$ and 2.0. For these cases, the flow field static pressure was not measured, and for calculations, the surface pressure on the cavity floor at those survey stations was assumed constant across the plane of survey. The total temperatures at those points in the reverse-flow boundary layer close to the wall that the temperature probe could not reach, were interpolated between measured values and the wall temperature.

The correlation of velocities with the error function profile (Appendix III) first required the location on each velocity profile of the point at which the velocity was one-half that at the free-stream edge of the mixing layer. This point at which $\frac{u}{u_\delta} = 0.5$ was the origin $y = 0$ of the correlation coordinate system and was determined from large scale plots of each velocity profile. Two quantities were to be found; the distance, x_o, from the front edge of the cavity to the effective origin of the mixing layer profiles and the coefficient, σ, describing the rate of growth in width of the mixing layer. These were chosen for the set of mixing layer profiles at and downstream of $\ell = 2$ in. at each test condition, to give the best fit between experimental and theoretical slope of velocity with vertical distance at the point $\frac{u}{u_\delta} = 0.5$.

The correlations of measured total temperature, with Crocco's temperature relation for the error function velocity profile, made use of the values of σ and x_o established from the velocity profiles. The additional quantities needed for this correlation were the total temperatures of the fluid at the free-stream and zero-velocity edges of the mixing layer. Experimental values of these temperatures were used.

3.4 PRECISION OF DATA

During the course of the test, the maximum deviations from the average operating conditions were within the following limits:

p_{o_∞}	T_{o_∞}	T_w/T_{o_∞}
±1.5 percent	±2 percent	±5.5 percent

There was negligible variation in Mach number from the stated conditions.

The estimated precision of measurements was as follows:

1. All pressure measurements: ±1 percent or ±0.004 psia, whichever is greater.
2. Model wall temperature: ±1 percent
3. Stilling chamber stagnation temperature: within 2 percent of the true value.

4. Flow field total temperature: The total temperature probes read consistently lower than the stilling chamber probe by an amount not greater than 1 percent, when free-stream readings were compared.

5. The model was aligned with the flow to within 0.3 deg.

SECTION IV
RESULTS AND DISCUSSION

The initial and boundary conditions for development of the cavity flow field are described in Figs. 4 and 5, and the data are presented in Tables II, III, and IV. The static pressure gradient along the forebody ahead of the cavity was zero for all cases (Fig. 4a), and the wall-to-free-stream temperature ratio (Fig. 4b) was constant in this region within ±0.04 in T_w/T_{o_∞}. The increase in static pressure ratio in the cavity over that of the forebody was associated with a weak shock wave system, which was observed in shadowgraphs. Along the floor of the cavity the wall temperature rises slightly going toward the downstream face; however, the static pressure remained essentially constant, indicating that the mixing layer developed in a region of zero streamwise pressure gradient. The only complete surface temperature distribution obtained at M_∞ = 8.09, that for T_w/T_{o_∞} = 0.45, is included to illustrate the close agreement between the forebody and cavity temperatures at this Mach number.

The velocity profiles of Fig. 5a indicate that the flow outside the boundary layer was of uniform velocity and that the boundary-layer thickness was of the order of 0.3 in. For these tests, with a cavity of 1.75-in. radial depth, the ratio of initial boundary-layer thickness to cavity depth was approximately 0.17. At M_∞ = 3.99 and 8.09, $T_w/T_{o_\infty} \cong 0.8$, the initial boundary layer was turbulent (Fig. 5b); however, at M = 8.09, $T_w/T_{o_\infty} \cong 0.4$, the boundary layer had not quite completed transition.

The schematic diagram of Fig. 6a illustrates the features of the cavity flow of the present experiment. The mixing layer develops from the initial boundary layer and proceeds across the cavity. At the cavity downstream face, a portion of the flow impinges on the cavity wall, causing the elevated surface pressures and temperatures in this region noted in Fig. 4. This impinging flow then proceeds toward the cavity floor and thence upstream as a recirculating reverse flow. A reverse-flow boundary layer forms between this recirculating flow and the cavity wall. The action of turbulent fluid in the lower velocity region of the mixing layer recovers the fluid which has circulated in the cavity and carries it along as part of the mixing layer until it again impinges on the aft face of the cavity. The oil flow photograph (Fig. 6b) shows the vortex nature of the recirculating flow. The oil streamer seen leaving the splitter plate was continuously blown back onto the aft face, thence toward the cavity floor, and back onto the splitter plate.

The velocity and total temperature profiles measured at $M_\infty = 8.09$, $\frac{T_w}{T_{o_\infty}} = 0.4$ (Fig. 7), show the features outlined above. The mixing layer, which has developed from the initial forebody boundary layer, the recirculating flow, and a boundary layer developed on the cavity floor are shown. The velocity profile between the mixing layer and the flow boundary layer is linear indicating a solid rotation vortex structure with velocity proportioned to distance from the center. The vortex is elongated along the cavity, and the oil flow photograph (Fig. 6b) indicates that it is confined to the downstream two-thirds of the cavity. The magnitude of the reverse-flow velocity reaches a maximum value nearly 0.5 times the free-stream velocity. In the upstream corner of the cavity, upstream of the vortex flow, is a region of inactive fluid (Fig. 6b).

The total temperature profiles of Fig. 7b supply information relative to the question of recirculating fluid temperature. Here, although the wall temperature is only 0.4 times the free-stream total temperature, the recirculating fluid remains at a temperature averaging $0.75\ T_{o_\infty}$ until the reverse-flow boundary layer is reached. It is within this cavity floor viscous layer that the largest part of the temperature drop from free-stream to wall value takes place. A summary of the experimental measured and calculated data at $\ell = 3$ for the above conditions is presented in Fig. 7c, and complete data are presented in Table V.

With regard to the assumption of Korst and Chow (Ref. 5) that the velocity profiles of a mixing layer can be adequately represented by the error function profile (Appendix III), the correlations of Fig. 8 indicate that this assumption is satisfactory even at hypersonic Mach numbers. Toward the outer region, which because of its higher velocity contributes most to the momentum of the flow, the maximum difference between the error function and the experimental velocities is about 5 percent.

The assumption that Crocco's linear relation between velocity and total temperature (Appendix I) is useful as an engineering approximation is also borne out by the experimental results (Fig. 9), although the form of the temperature distribution does not follow the form of the theory. The experimental data follow the form of the total temperature distribution in a boundary layer of air ($Pr \approx 0.7$) over an insulated plate (Appendix I and Ref. 8), in that there is a migration of energy to the outer layers of fluid, resulting in an excess of total temperature above either the wall temperature or the free-stream total temperature. The errors involved, however, with using the Crocco relation as an approximation to the total temperature distribution in the present case are less than 7 percent.

The manner in which heat transfer from the outer stream to the cavity wall takes place involves both the mixing layer and the reverse-flow boundary layer. High temperature fluid is received into the cavity from the mixing layer at the cavity downstream face. This fluid then passes, in part, into the cavity floor boundary layer, and heat is transferred from the fluid to the cavity wall. The cooler reverse-flow boundary-layer fluid then passes up into, and becomes part of, the mixing layer near the upstream face of the cavity. As the mixing layer proceeds downstream, energy is transferred across the mixing layer from the free stream to the cooler reverse-flow fluid. The greatest resistance to the flow of heat is the reverse-flow boundary layer, which requires a large temperature difference to transfer an amount of heat which the mixing layer can transfer internally with very little temperature drop. It is for this reason that the temperature is nearly constant across the mixing layer and recirculating flow, dropping rapidly only in the reverse-flow boundary layer.

The values of σ used in the correlations of mixing layer velocity with the error function velocity profile (Fig. 8) were all near 12, as shown in Fig. 10. This is an accepted value of σ for subsonic flow (Ref. 9). The summary of jet-spreading data presented in Ref. 9 indicates that, rather than 12, the value of σ at M_∞ = 3.99 should have been about 25, and that it should be even higher is suggested by the data of Cary presented in this reference. In Ref. 10 a comparison is presented of a relation for σ suggested by Korst and a relation proposed by Abramovich. The Korst equation gives σ values at M_∞ = 4 and 8 of 23 and 34, respectively, whereas the Abramovich relation gives 17.5 and 20.5. The experimental work of Ref. 11 indicated that when shock wave disturbances were located near the origin of the mixing layer, the value of σ dropped sharply from its value in disturbance-free flow. The presence of the weak shock wave system at the beginning of the cavity flow region may have affected the present experimental results in a similar manner.

SECTION V
CONCLUSIONS

An experimental investigation of turbulent flow over a cavity in an aerodynamic surface has been conducted. The test was carried out at

Mach numbers 3.99 and 8.09, with Reynolds numbers based on free-stream conditions and length of body ahead of the cavity of 8.0×10^6 and 11.0×10^6, respectively. Two conditions of wall-to-free-stream stagnation temperature ratio, 0.4 and 0.8, were tested at $M_\infty = 8.09$, whereas at $M_\infty = 3.99$, the temperature ratio was 0.75. For all tests, the ratio of initial boundary-layer thickness to cavity depth was approximately 0.2, and there was negligible model wall temperature or pressure gradient upstream of the cavity. Within this range of variables, the following conclusions can be made:

1. At $M_\infty = 8.09$, with the wall temperature only 0.4 times the free-stream stagnation temperature, the recirculating fluid total temperature averaged 0.75 times the free-stream value. The further decrease in temperature from that of the recirculating fluid to that at the wall took place across the thin, reverse-flow boundary layer along the cavity floor.

2. The compressible-flow experimental velocities correlated well with the theoretical incompressible-flow error function profile of Goertler.

3. Crocco's linear relation between velocity and total temperature adequately described the total temperature variation across the mixing layer.

4. The mixing zone similarity parameter, σ, was near 12 regardless of Mach number or wall temperature ratio.

REFERENCES

1. Crocco, L. and Lees, L. "A Mixing Theory for Interaction between Dissipative Flows and Nearby Isentropic Streams." Journal of the Aeronautical Sciences, Vol. 19, No. 10. October 1952, pp. 649-676.

2. Glick, Herbert S. "Modified Crocco-Lees Mixing Theory for Supersonic Separated and Reattaching Flows." Guggenheim Aeronautical Laboratory, California Institute of Technology Memorandum No. 53 (AD239560), May 1960.

3. Chapman, Dean R. "A Theoretical Analysis of Heat Transfer in Regions of Separated Flow." NACA TN 3792, October 1956.

4. Larson, Howard K. "Heat Transfer in Separated Flow." Journal of the Aero Space Sciences, Vol. 26, No. 11, November 1959, pp. 731-738.

5. Korst, H. H. and Chow, W. L. "Non-Isoenergetic Turbulent (Pr_t = 1) Jet Mixing between Two Compressible Streams at Constant Pressure." University of Illinois Engineering Experiment Station, ME-TN-393-2, April 1965.

6. Larson, R. E., Scott, C. J., Elgin, D. R., and Seiver, R. E. "Turbulent Base Flow Investigations at Mach Number 3." Rosemount Aeronautical Laboratories, University of Minnesota, Research Report No. 183, July 1962.

as amended

7. Test Facilities Handbook (5th Edition). "von Kármán Gas Dynamics Facility, Vol. 4." Arnold Engineering Development Center, July 1963.

8. Shapiro, Ascher H. The Dynamics and Thermodynamics of Compressible Fluid Flow, Vol. II. The Ronald Press Co., New York, 1954.

9. Maydew, R. C. and Reed, J. F. "Turbulent Mixing of Compressible Free Jets." AIAA Journal, Vol. 1, No. 6, June 1963, pp. 1443-1444.

10. Bauer, R. C. "Characteristics of Axisymmetric and Two-Dimensional Isoenergetic Jet Mixing Zones." AEDC-TDR-63-253 (AD426116), December 1963.

11. Cary, Boyd. "An Optical Study of Two-Dimensional Jet Mixing." Doctoral Thesis, University of Maryland, 1954.

12. Schlichting, Hermann. Boundary Layer Theory, Fourth Edition. McGraw-Hill Book Company, Inc., New York, 1960.

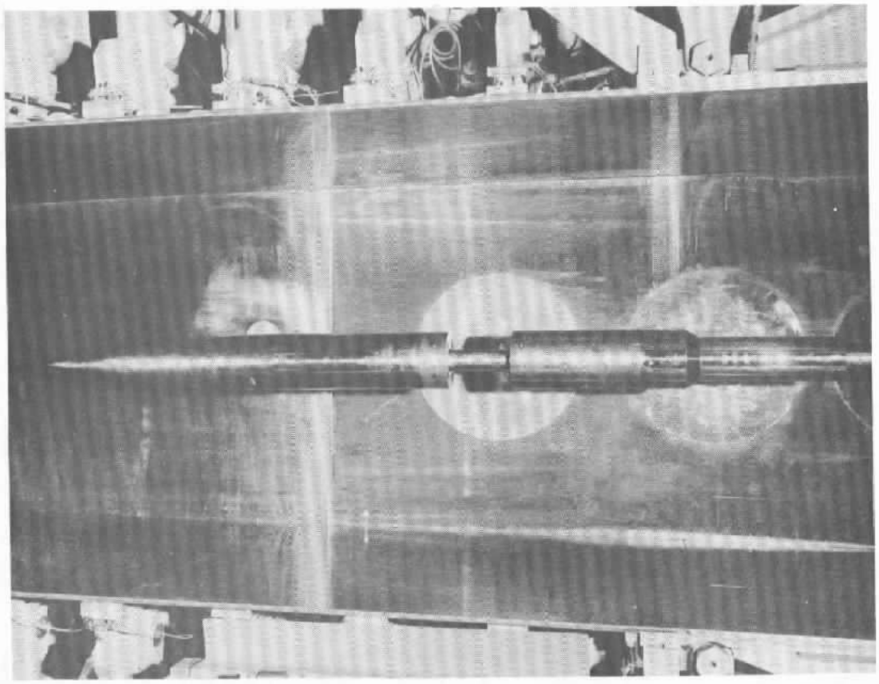

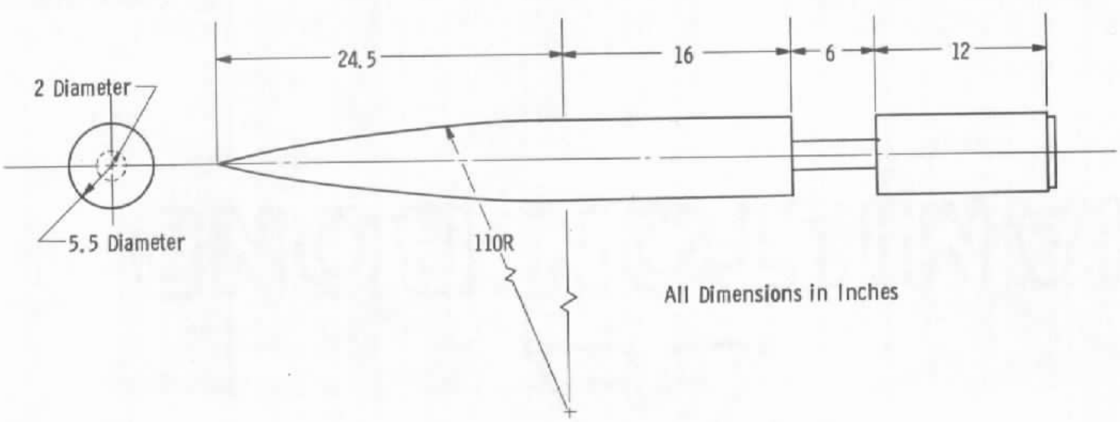

Fig. 1 Wind Tunnel Model

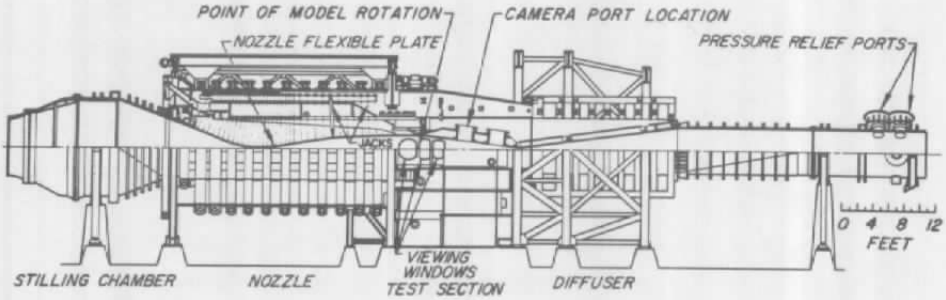

Assembly

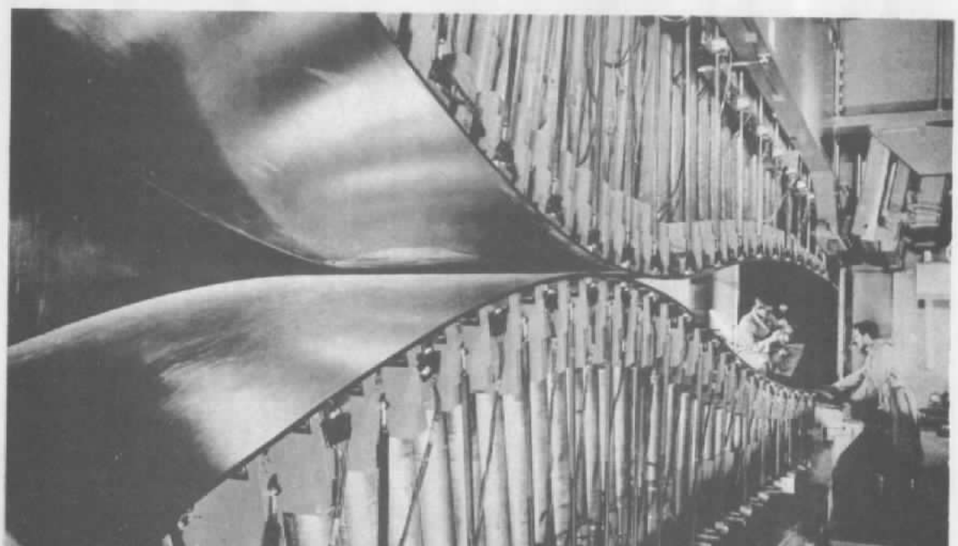

a. Tunnel A

Fig. 2 Wind Tunnels

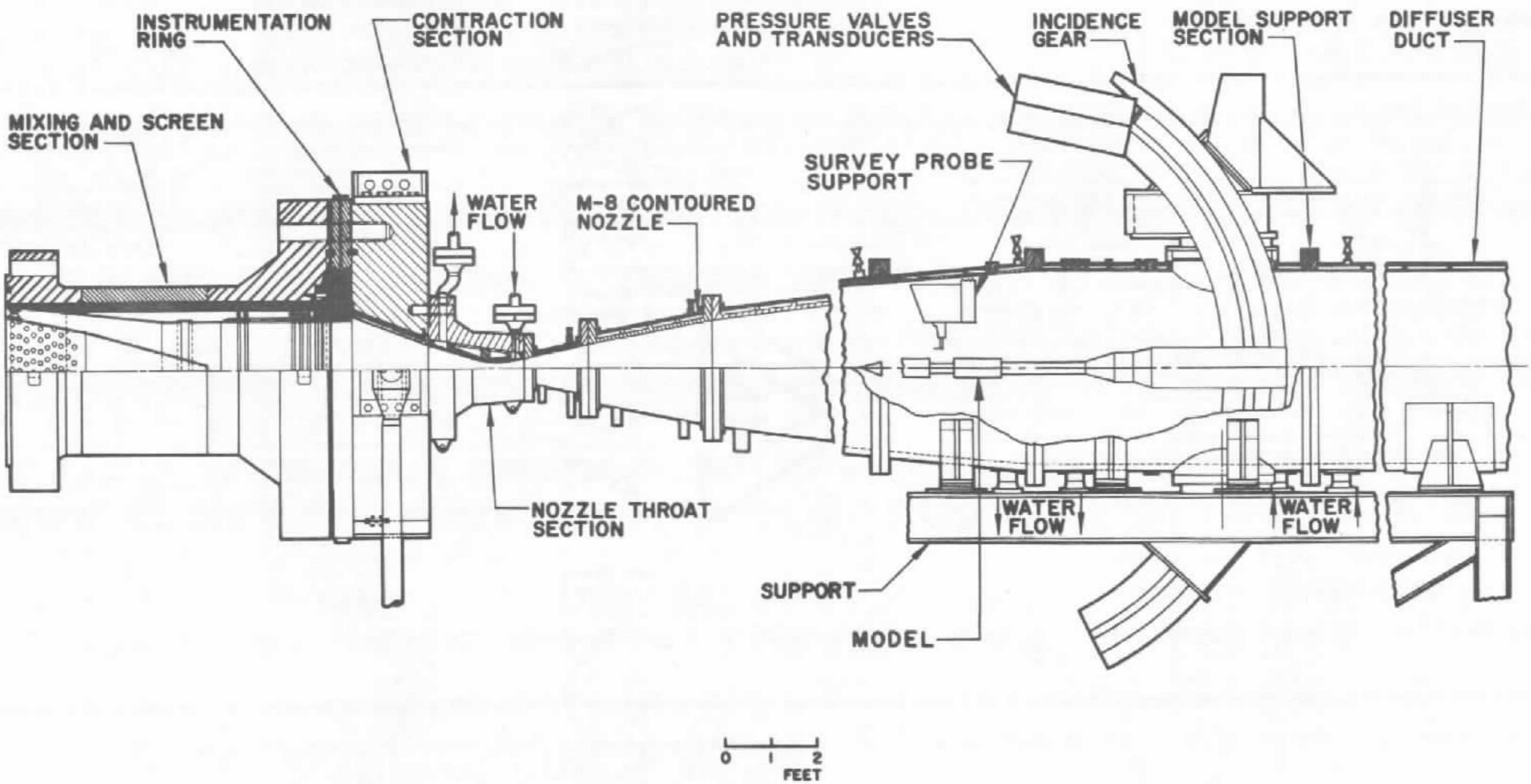

b. Tunnel B

Fig. 2 Concluded

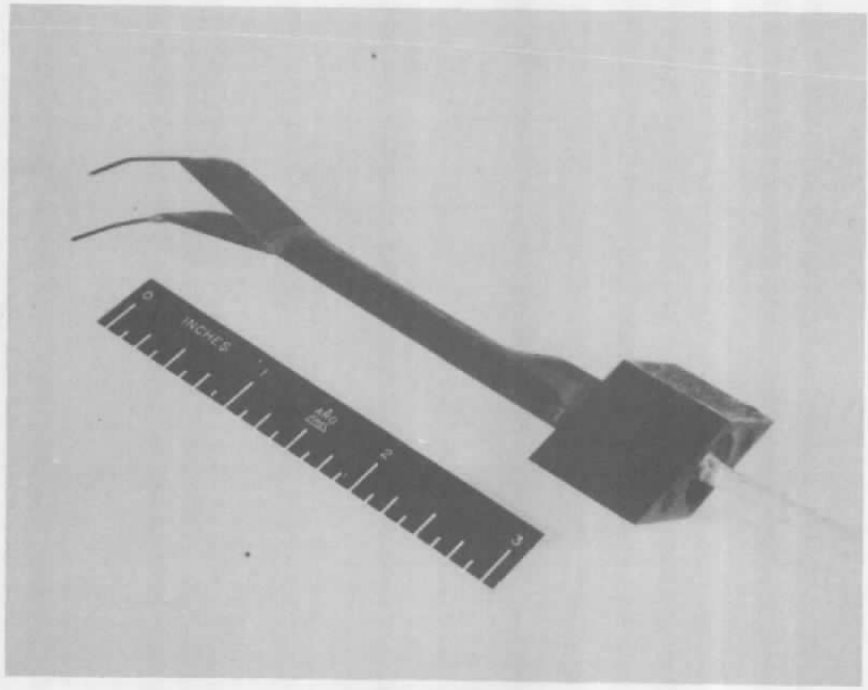

a. Pitot and Static Probes

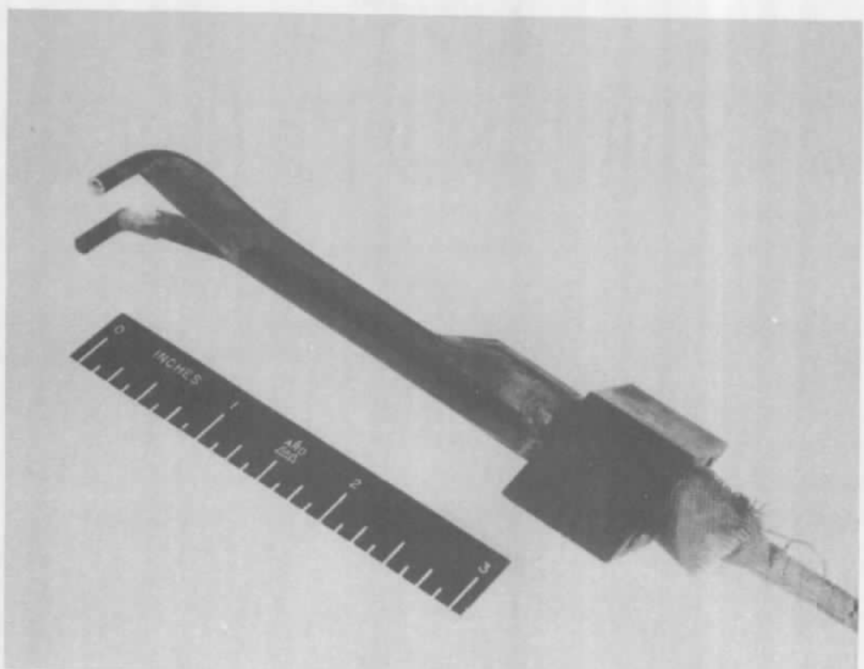

b. Total Temperature Probe

Fig. 3 Flow Survey Probes

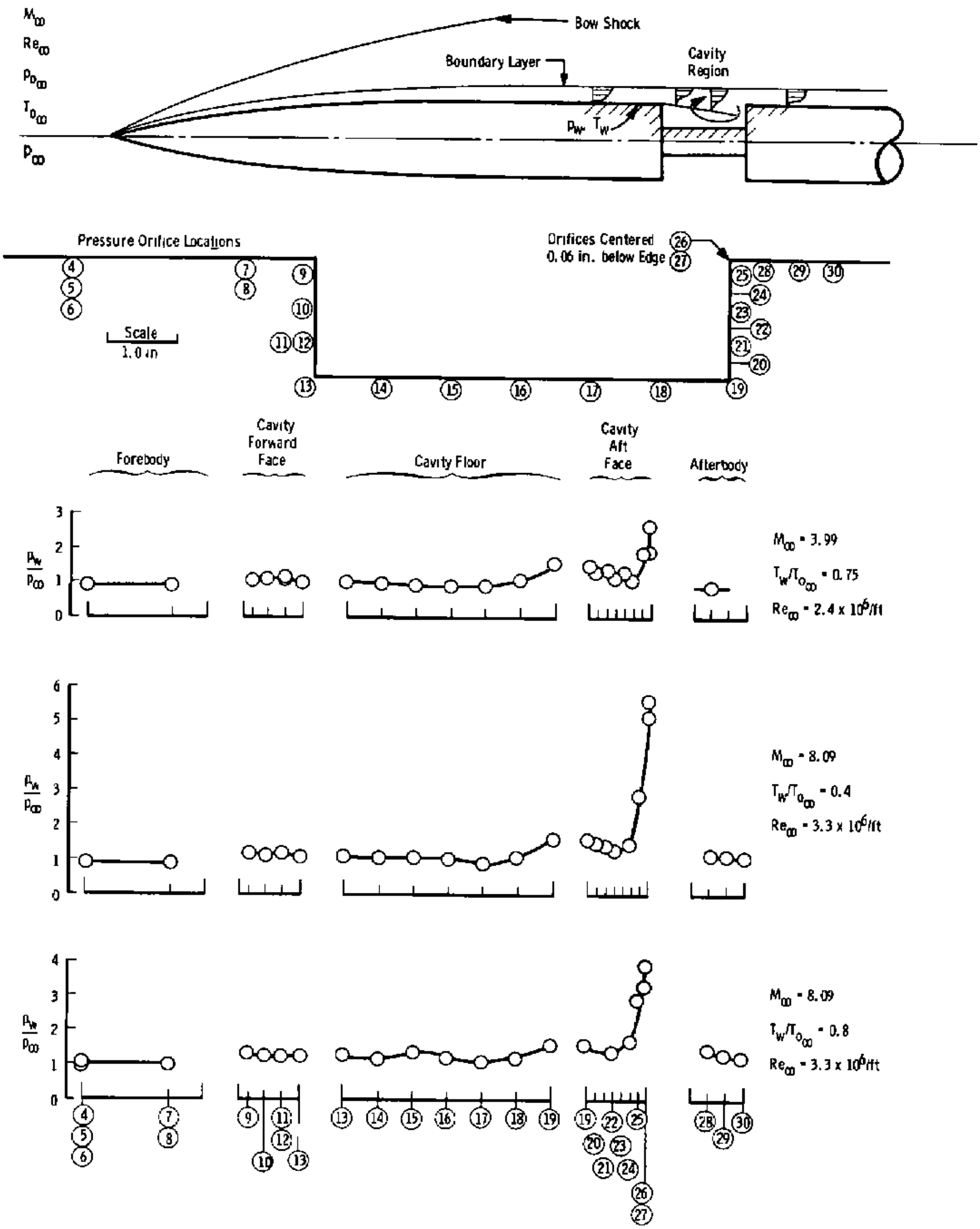

a. Surface Pressure

Fig. 4 Surface Pressure and Temperature

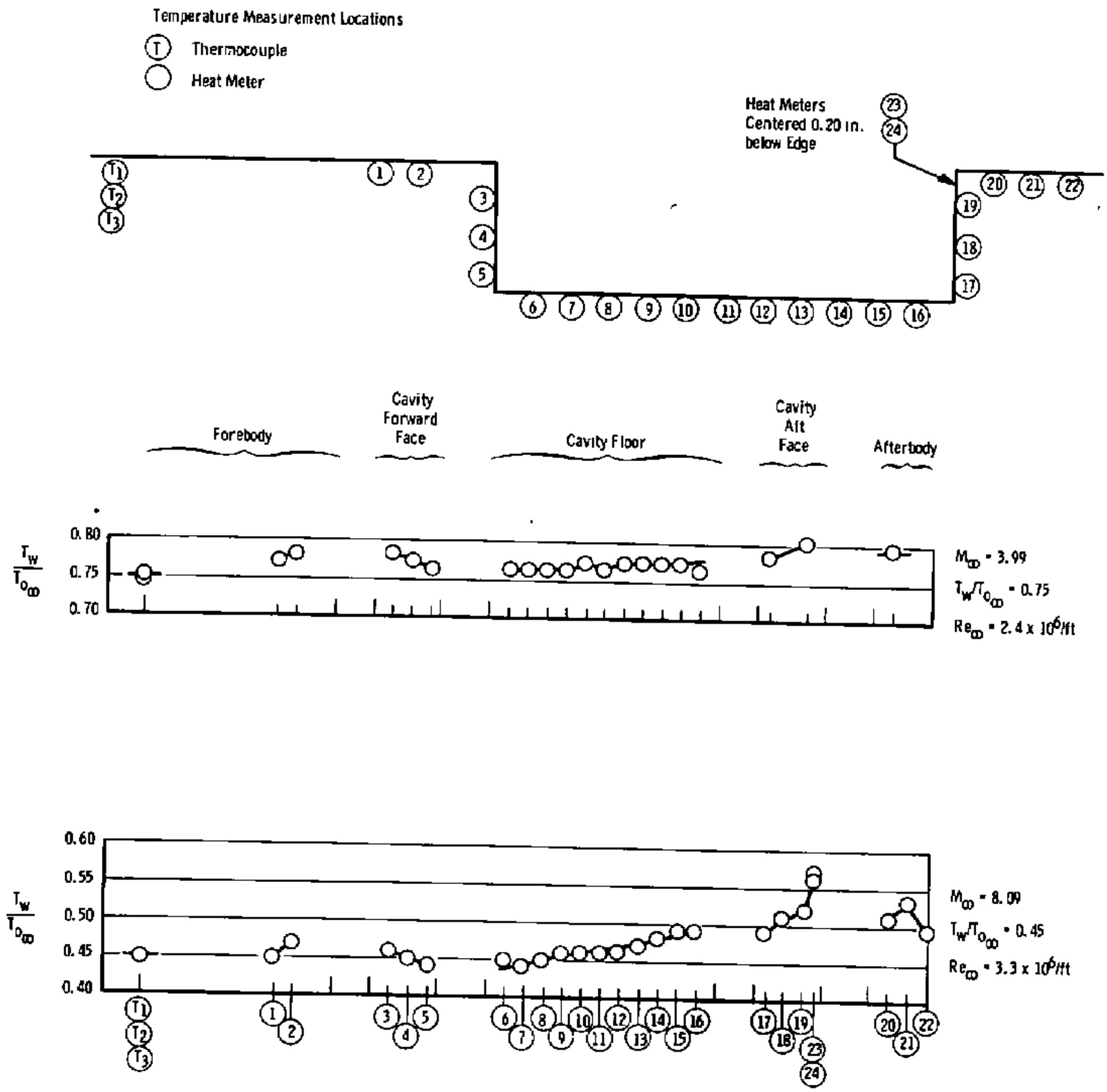

b. Surface Temperature

Fig. 4 Concluded

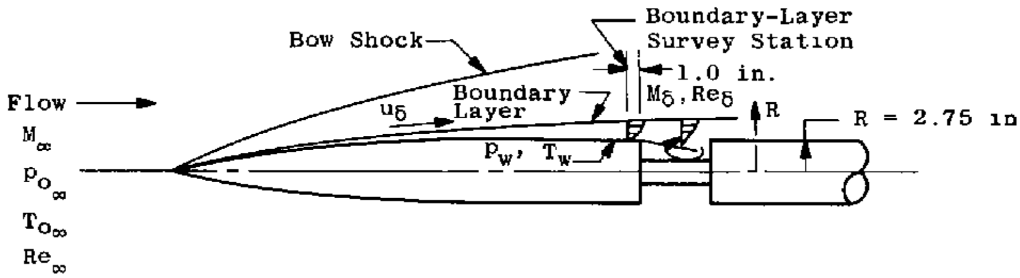

$M_\infty = 3.99$	$M_\infty = 8.09$	$M_\infty = 8.09$
$p_{o_\infty} = 37$ psia	$p_{o_\infty} = 803$ psia	$p_{o_\infty} = 802$ psia
$T_{o_\infty} = 673^oR$	$T_{o_\infty} = 1345^oR$	$T_{o_\infty} = 1326^oR$
$Re_\infty \cong 2.3 \times 10^6$/ft	$Re_\infty \cong 3.3 \times 10^6$/ft	$Re_\infty \cong 3.3 \times 10^6$/ft
$T_w/T_{o_\infty} = 0.75$	$T_w/T_{o_\infty} = 0.40$	$T_w/T_{o_\infty} = 0.80$
$p_w = 0.229$ psia	$p_w = 0.070$ psia	$p_w = 0.076$ psia
$M_\delta = 3.99$	$M_\delta = 7.71$	$M_\delta = 7.53$
$Re_\delta = 2.3 \times 10^6$/ft	$Re_\delta = 2.6 \times 10^6$/ft	$Re_\delta = 2.6 \times 10^6$/ft

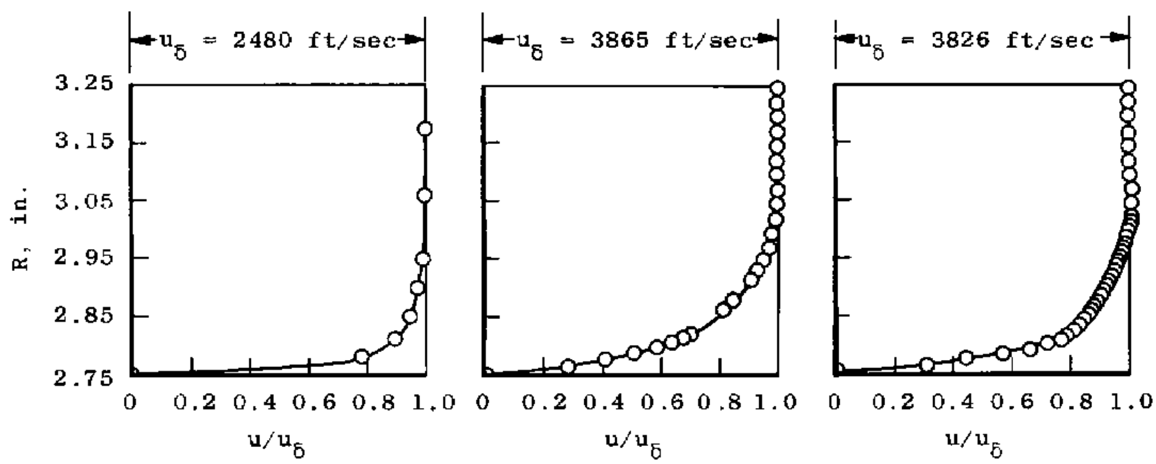

a. Velocity Profiles

Fig. 5 Forebody Velocity Profiles

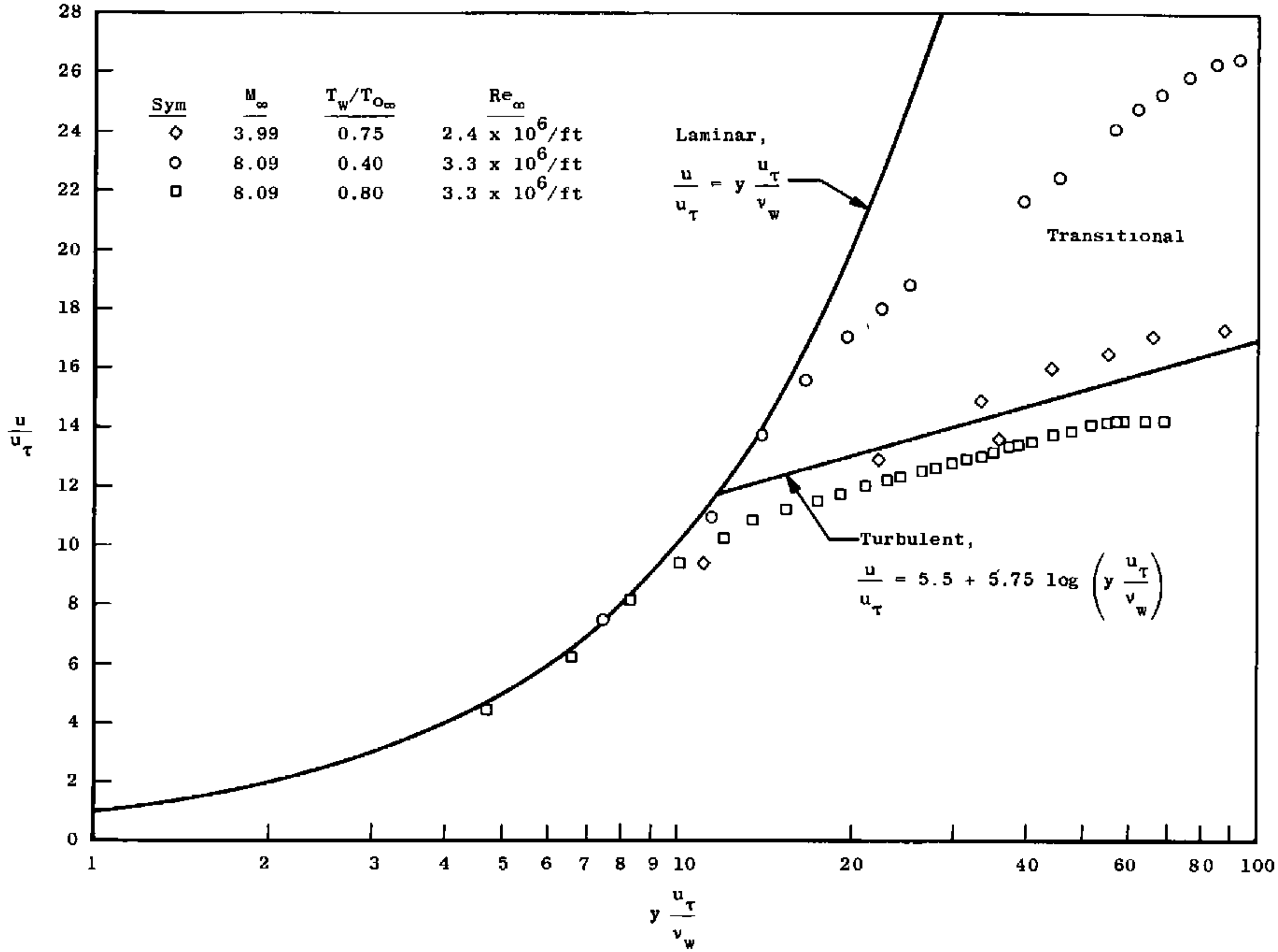

b. Comparison of Experimental Profiles with Universal Velocity Profile

Fig. 5 Concluded

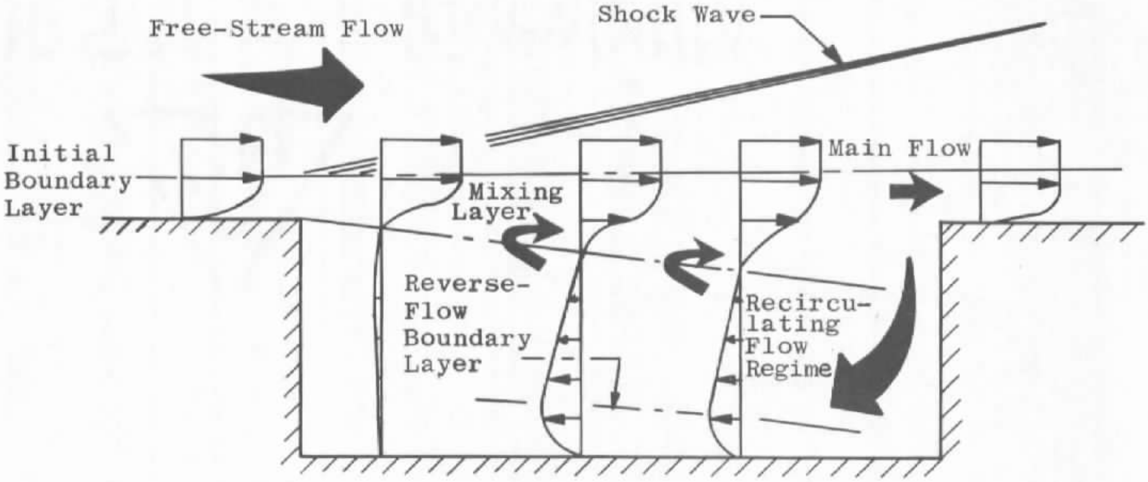

a. Schematic Diagram

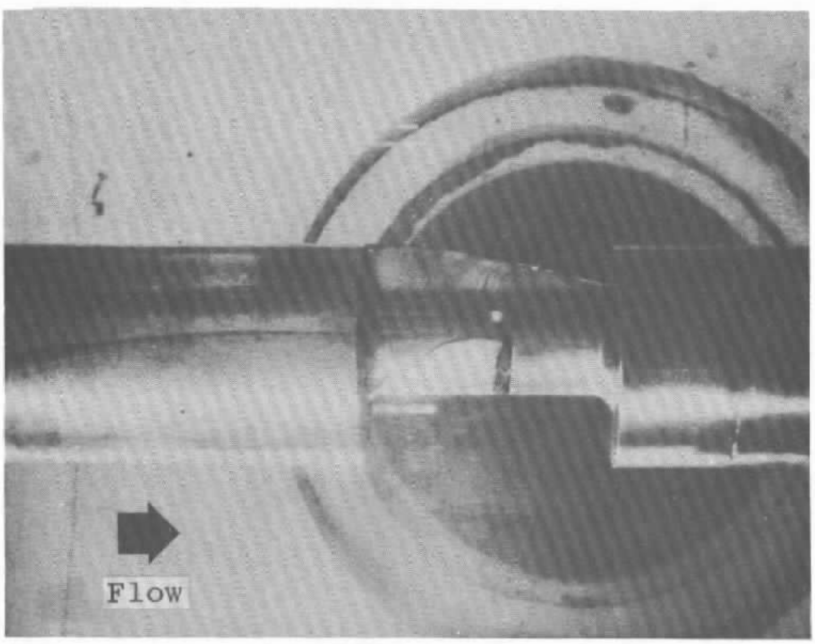

b. Oil Flow Photograph of Cavity Flow Region

Fig. 6 Main Features of Experimental Cavity Flow

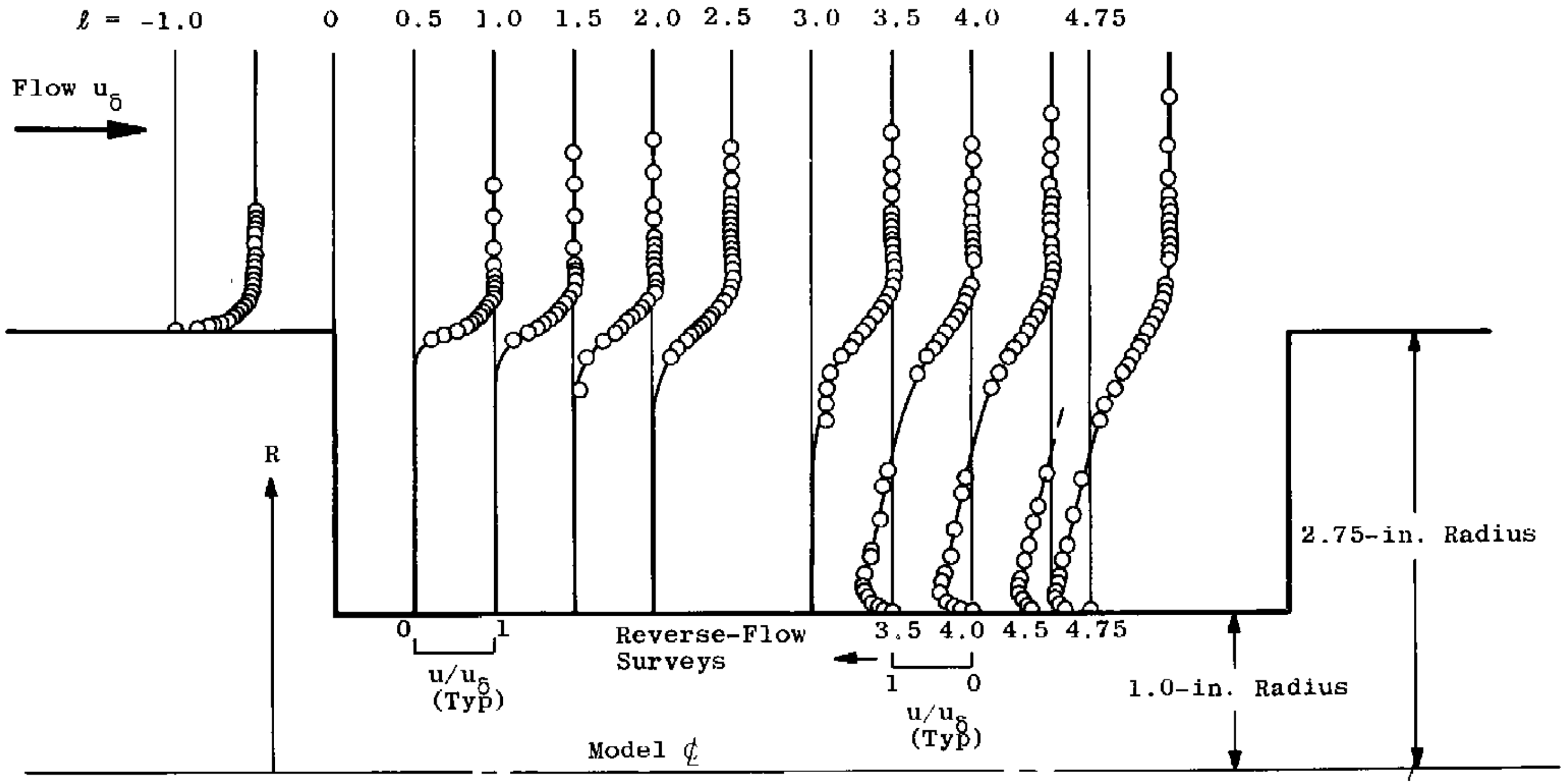

a. Velocity Profiles

Fig. 7 Velocity and Total Temperature Profiles of Cavity Flow, $M_\infty = 8.09$, $T_w/T_{o_\infty} = 0.40$, and $Re_\infty = 3.3 \times 10^6$ ft

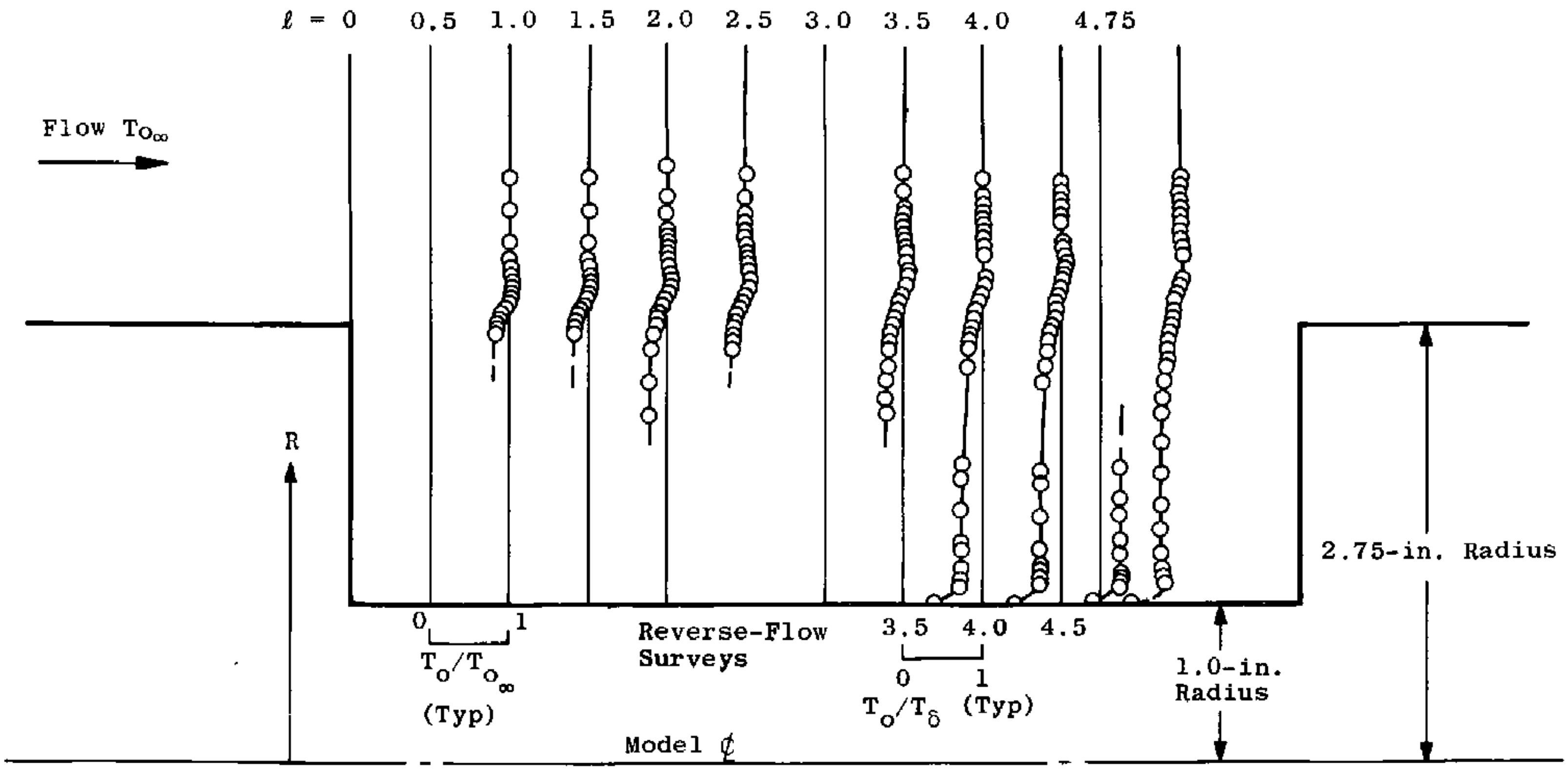

b. Total Temperature Profiles

Fig. 7 Continued

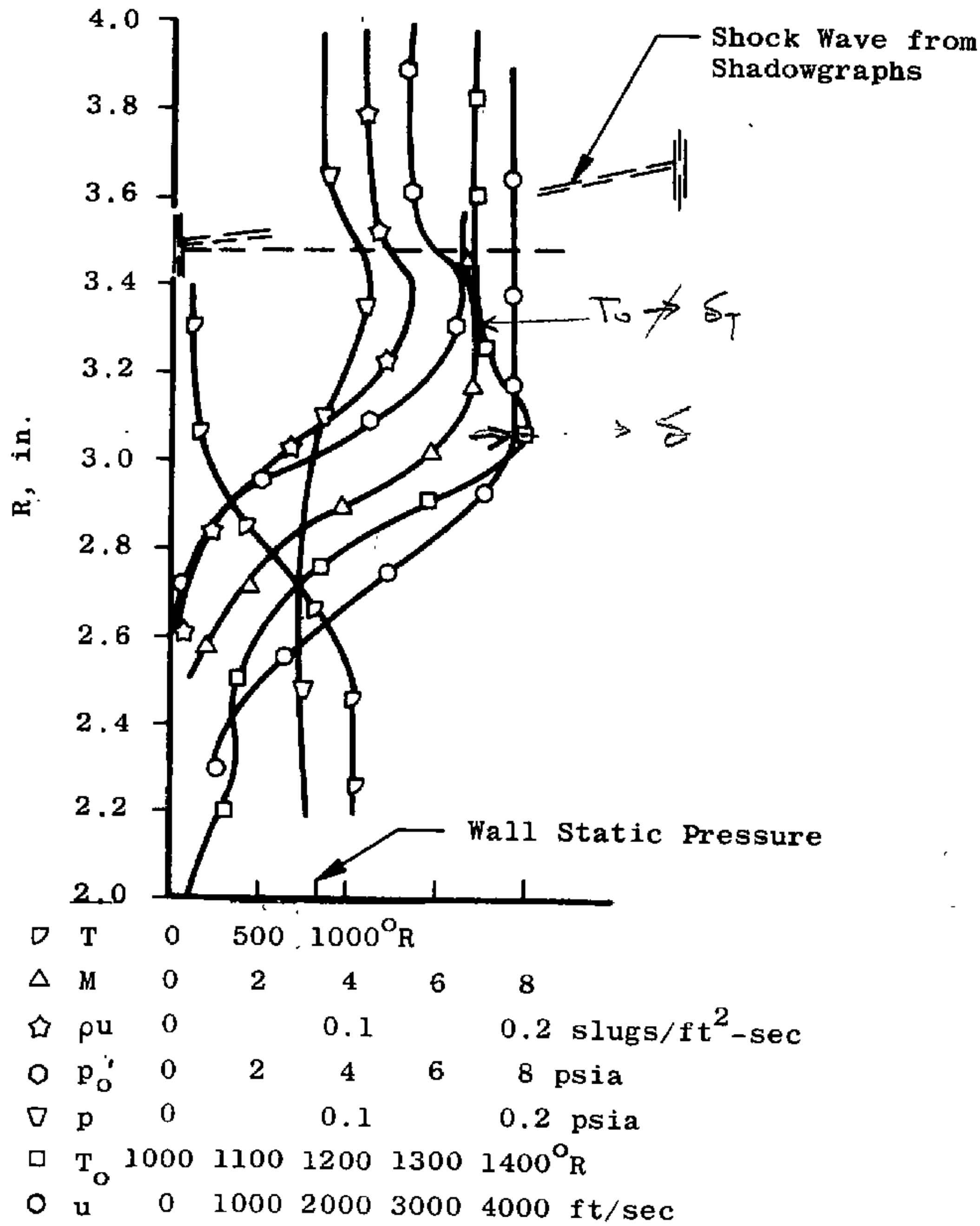

c. Summary of Measured and Calculated Survey Data, $\ell = 3$, $M_\infty = 8.09$, $T_w/T_{o_\infty} = 0.4$, and $Re_\infty = 3.3 \times 10^6$/ft

Fig. 7 Concluded

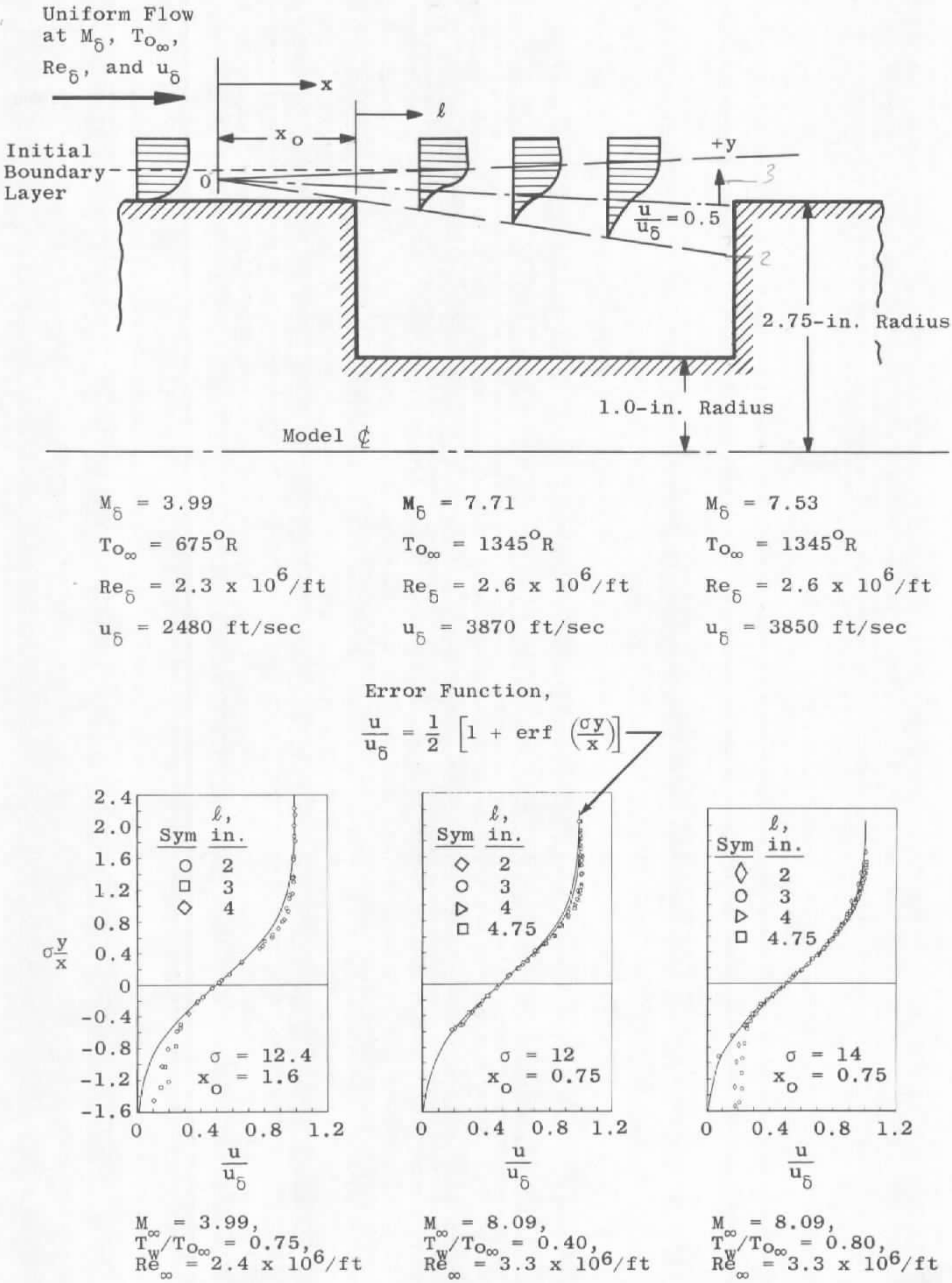

Fig. 8 Correlation of Experimental Velocity Profiles with the Error Function Profile

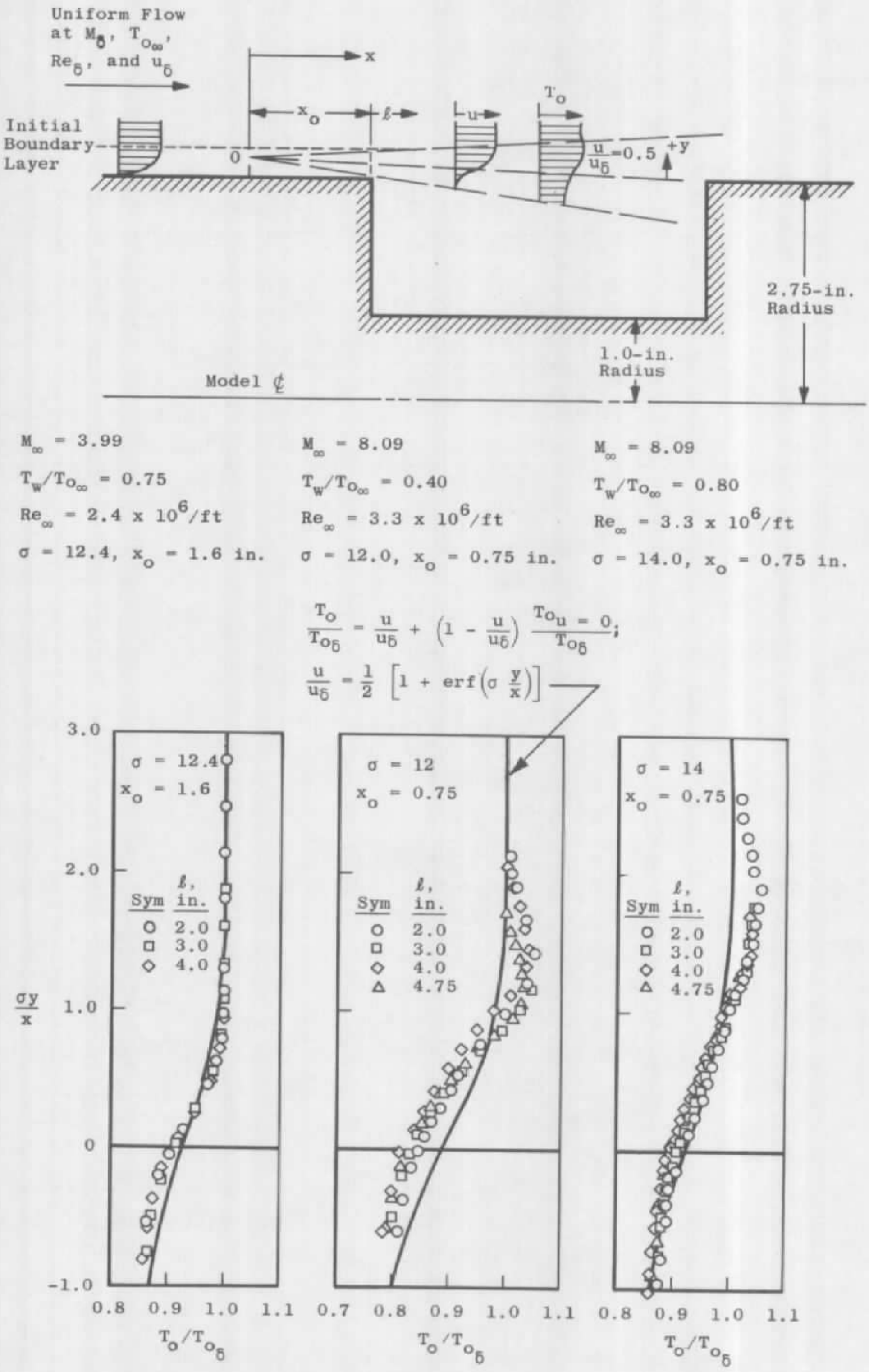

Fig. 9 Correlation of Experimental Total Temperature Profiles with Crocco Relation Derived with Error Function Velocity Profile

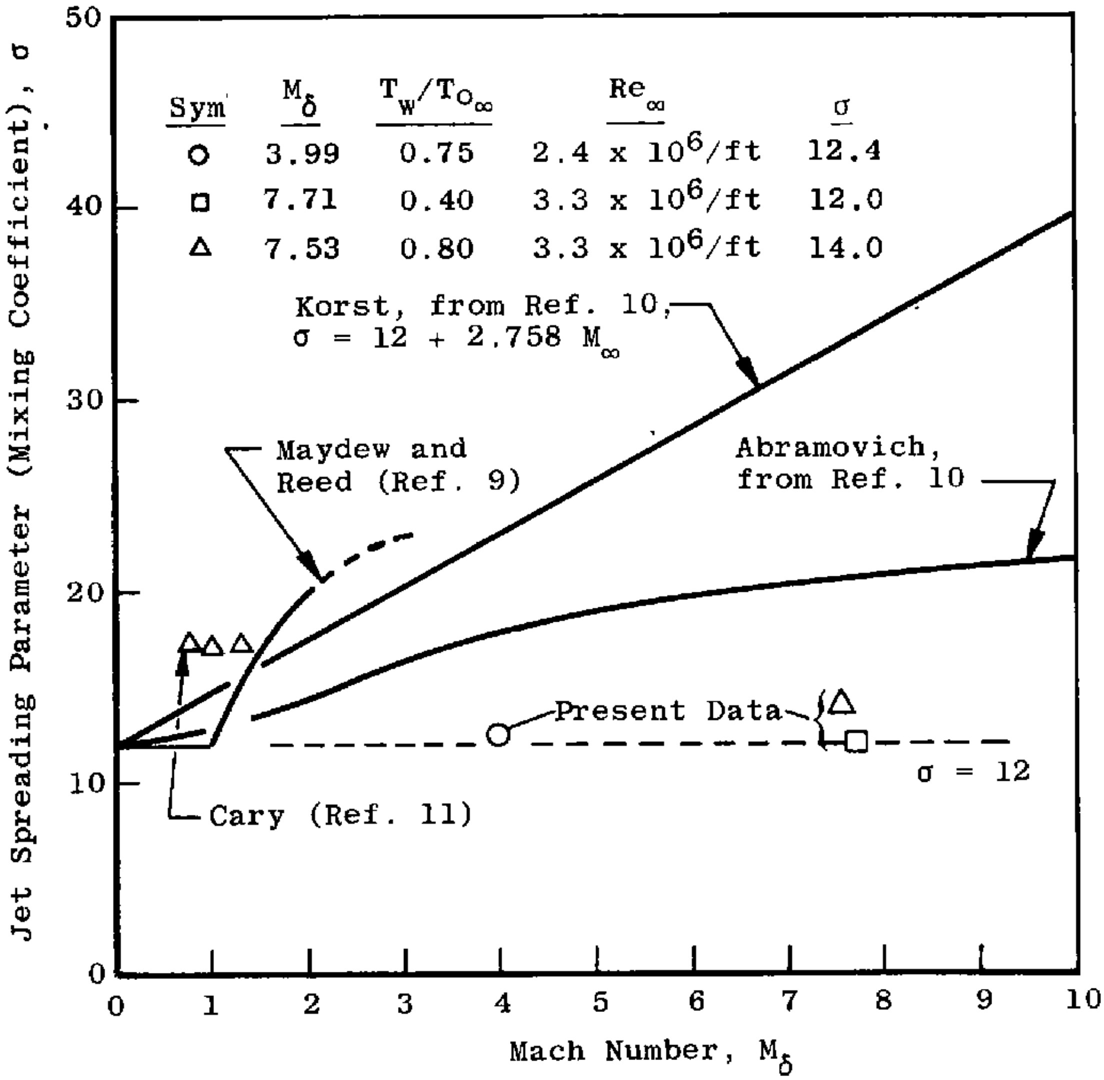

Fig. 10 Comparison of Experimental σ Values with Proposed Theoretical Relations and Other Data

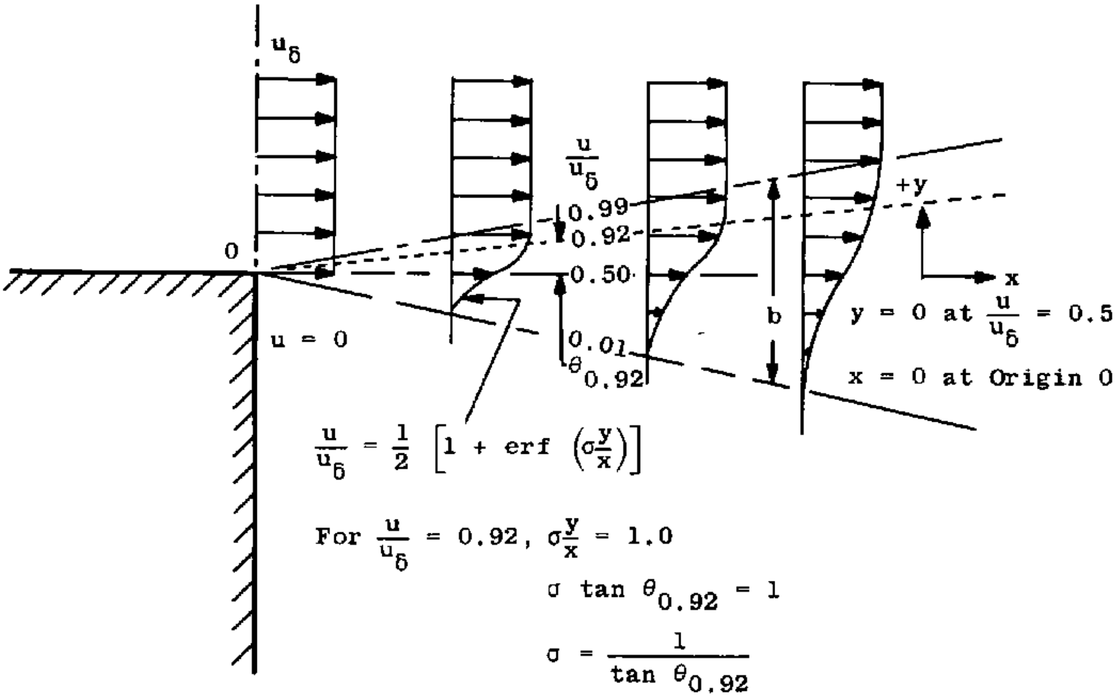

a. No Initial Boundary Layer

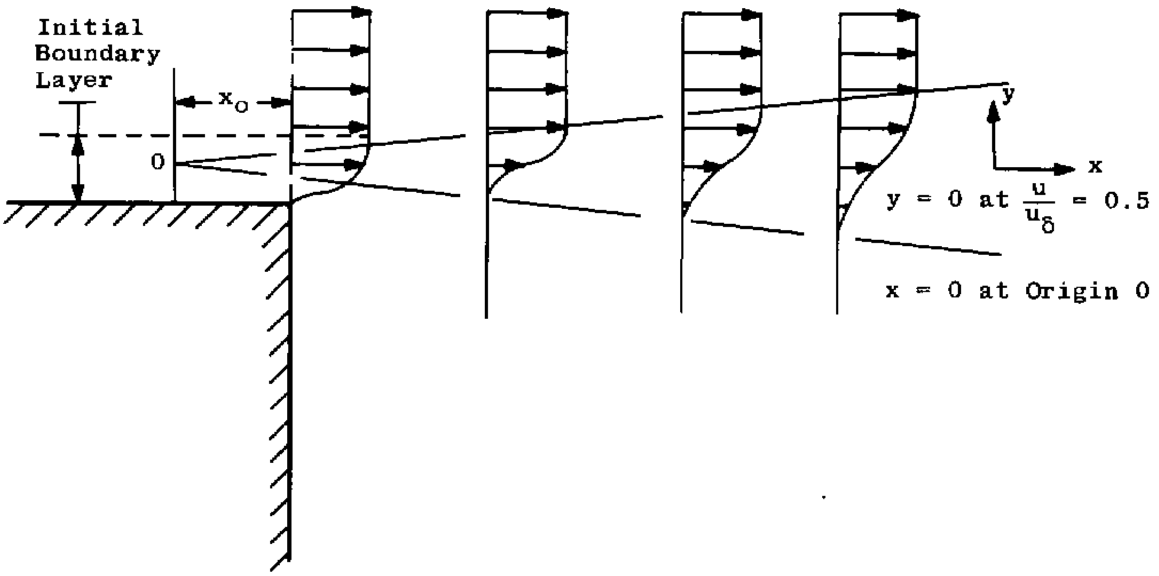

b. Initial Boundary Layer Present

Fig. 11 Free Mixing Layers with and without Initial Boundary Layer

TABLE I
SUMMARY OF MEASUREMENTS

Test Condition		Wind Tunnel		Model Surface		Flow Field			Survey Location
M_∞	T_w/T_{o_∞}	p_{o_∞}	T_{o_∞}	p_w	T_w	p_o'	p	T_o	ℓ, in.
3.99	0.75	x	x	x	x				
		x	x			x		x	0.8
		x	x			x		x	2.0
		x	x			x		x	3.0
		x	x			x		x	4.0
		x	x			x			Forebody
8.09	0.45	x	x		x				
8.09	0.40	x	x	x	(Forebody Only)				
		x	x			x	x	x	0.5
		x	x			x	x	x	1.0
		x	x			x		x	1.5
		x	x			x		x	2.0
		x	x			x	x	x	3.0
		x	x			x	x	x	3.5
		x	x			x	x	x	4.0
		x	x			x	x	x	4.75
		x	x			x	x		Forebody
						(Reverse-Flow Survey)			
		x	x			x	x	x	3.5
		x	x			x	x	x	4.0
		x	x			x	x	x	4.5
		x	x			x	x	x	4.75
8.09	0.80	x	x	x	(Forebody Only)				
		x	x			x	x		0.1
		x	x					x	0.2
		x	x			x	x	x	1.0
		x	x			x	x	x	2.0
		x	x			x	x	x	3.0
		x	x			x	x	x	4.0
		x	x			x	x		4.75
		x	x					x	5.0
		x	x			x	x	x	Forebody

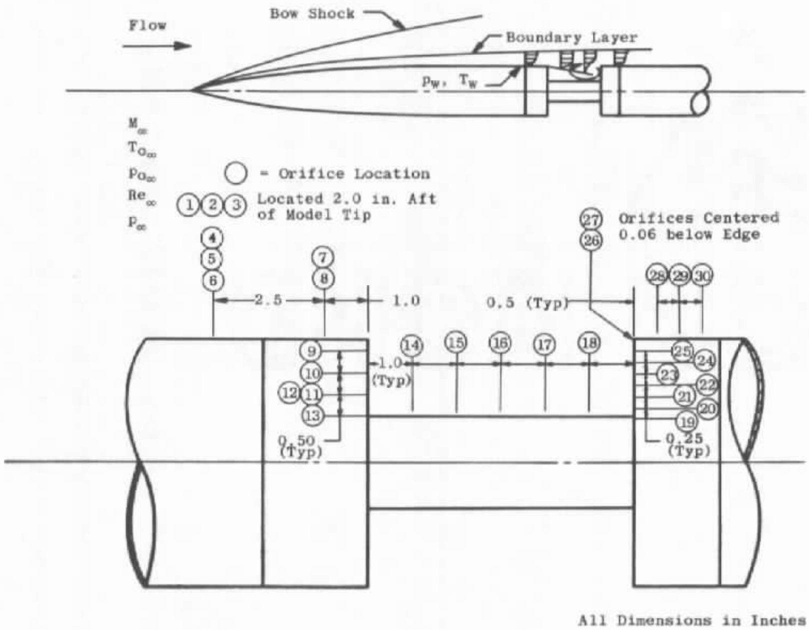

Nomenclature and Surface Pressure Orifice Location for Surface Pressure Data of Table II

TABLE II
SURFACE PRESSURES

p_w/p_∞							
Orifice No.	A	B	C	Test Condition	A	B	C
1	2.09	5.09	4.78	M_∞	3.99	8.09	8.09
2	2.17	5.20	4.98	T_w/T_{o_∞}	0.75	0.40	0.80
3	2.07	4.87	---				
4	0.91	0.89	0.93	Re_∞, ft^{-1}	2.4×10^6	3.3×10^6	3.3×10^6
5	0.96	0.89	1.04				
6	0.93	0.90	0.97	p_{o_∞}, psia	37.3	800	804
7	0.92	0.88	1.01	T_{o_∞}, °R	673	1343	1322
8	0.93	0.92	0.98	p_∞, psia	0.249	0.076	0.076
9	1.03	1.22	1.38				
10	1.07	1.17	1.24				
11	1.16	1.21	1.24				
12	1.06	1.21	1.25				
13	1.00	1.14	1.25				
14	1.00	1.15	1.16				
15	0.92	1.12	1.37				
16	0.91	1.04	1.21				
17	0.94	0.92	1.04				
18	1.10	1.15	1.22				
19	1.55	1.65	1.58				
20	1.28	1.54	---				
21	1.38	1.44	---				
22	1.16	1.32	1.38				
23	1.28	---	---				
24	1.07	1.55	1.67				
25	1.89	2.87	2.88				
26	2.70	5.62	3.32				
27	1.96	5.17	3.95				
28	0.90	1.18	1.41				
29	---	1.14	1.24				
30	---	1.11	1.21				

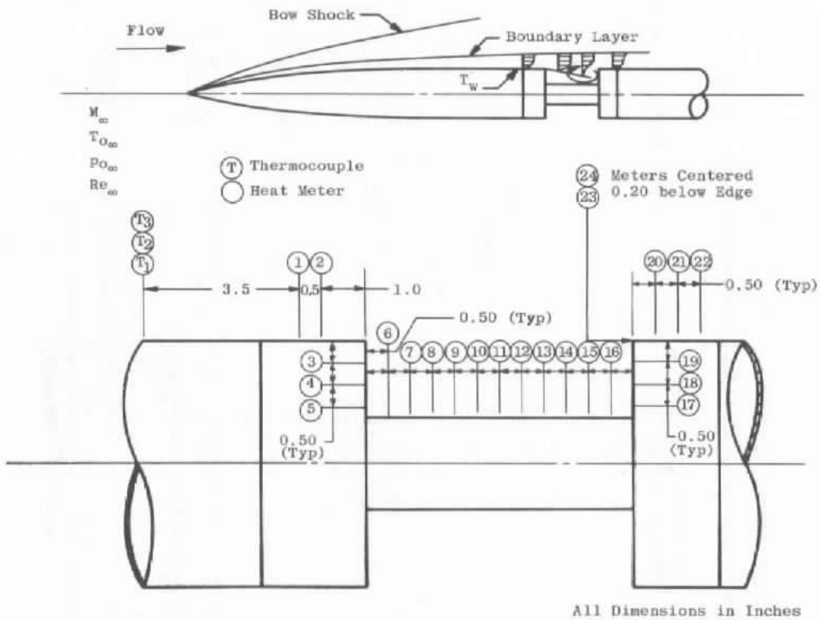

Nomenclature, Thermocouple and Heat Meter Locations for Surface Temperature Data of Table III

TABLE III
SURFACE TEMPERATURES

T_w/T_{o_∞}					
Thermocouple No.	A	B	Test Condition	A	B
T_1	0.74	0.45	M_∞	3.99	8.09
T_2	0.75	---	Nominal T_w/T_{o_∞}	0.75	0.45
T_3	0.75	---	Re_∞, ft^{-1}	2.4×10^{-6}	3.3×10^{6}
1	0.77	0.45	p_{o_∞}, psia	37.0	800
2	0.78	0.47	T_{o_∞}, °R	678	1367
3	0.78	0.46			
4	0.77	0.45			
5	0.76	0.44			
6	0.76	0.45			
7	0.76	0.44			
8	0.76	0.45			
9	0.76	0.46			
10	0.77	0.46			
11	0.76	0.46			
12	0.77	0.46			
13	0.77	0.47			
14	0.77	0.48			
15	0.77	0.49			
16	0.76	0.49			
17	0.78	0.49			
18	---	0.51			
19	0.80	0.52			
20	0.79	0.51			
21	---	0.53			
22	---	0.49			
23	---	0.56			
24	---	0.57			

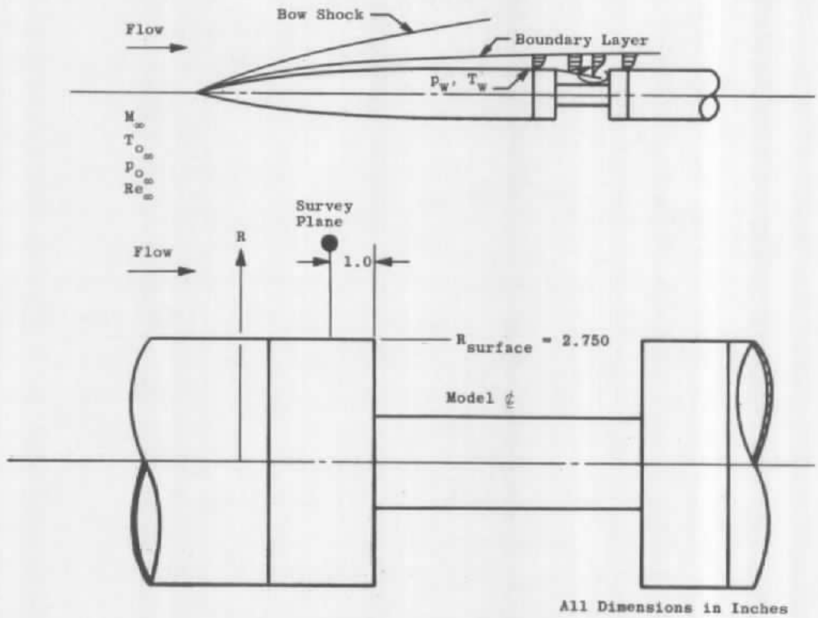

Nomenclature for Forebody Boundary-Layer Survey Data of Table IV

TABLE IV
FOREBODY BOUNDARY-LAYER SURVEY DATA

$M_\infty = 3.99$

$T_W/T_{O_\infty} = 0.75$

$Re_\infty = 2.4 \times 10^6$ /ft

$p_{O_\infty} = 37.0$ psia

$T_{O_\infty} = 673°R$

				Crocco Relation	
R, in.	p_o', psia	p_w, psia	M	T_o, °R	u, ft/sec
2.780	1.53	0.230	2.20	637	1939
2.810	2.57	↓	2.89	656	2222
2.850	3.36		3.32	664	2342
2.900	3.91		3.59	668	2403
2.950	4.41		3.82	671	2450
3.060	4.80		3.99	673	2480
3.175	4.76		↓	↓	↓
3.290	4.85				
3.490	4.77				
3.700	4.82	0.230	3.99	673	2480

TABLE IV (Continued)

Forebody Velocities

$M_\infty = 8.09$ $Re_\infty = 3.3 \times 10^6/ft$

$T_w/T_{o_\infty} = 0.40$ $p_{o_\infty} = 803$ psia

$T_{o_\infty} = 1345°R$

				Crocco Relation	
R, in.	p_o', psia	p_w, psia	M	T_o, °R	u, ft/sec
2.766	0.103	0.070	0.86	751	1010
2.777	0.169	↓	1.25	850	1487
2.785	0.266		1.61	932	1872
2.793	0.349		1.89	992	2166
2.802	0.440		2.14	1043	2405
2.810	0.506		2.32	1075	2460
2.818	0.576		2.49	1102	2684
2.860	0.98		3.25	1192	3118
2.877	1.21		3.62	1222	3253
2.910	1.82		4.44	1270	3495
2.927	2.23		4.94	1286	3567
2.945	2.67		5.41	1303	3648
2.967	3.40		6.11	1322	3738
2.993	4.13		6.75	1333	3786
3.018	4.63		7.14	1341	3827
3.043	4.87		7.32	1345	3850
3.068	5.01		7.45	↓	3852
3.093	5.09		7.48		3852
3.118	5.14		7.52		3850
3.143	5.19		7.57		3847
3.168	5.23		7.60		3856
3.193	5.26		7.62		3860
3.216	5.28		7.63		3860
3.241	5.29		7.65		3850
3.267	5.31		7.65		3850
3.317	5.32		7.67		3855
3.417	5.34		7.68		3855
3.517	5.38		7.71		3865
3.616	5.38	↓	7.71	↓	3865
3.768	5.39	0.070	7.71	1345	3865

TABLE IV (Continued)

Forebody Velocities

$M_\infty = 8.09$

$T_W/T_{O_\infty} = 0.80$

$Re_\infty = 3.3 \times 10^6/ft$

$p_{O_\infty} = 802$ psia

$T_{O_\infty} = 1326°R$

R, in.	p_O', psia	p_W, psia	M	T_O, °R	u, ft/sec
2.766	0.107	0.076	0.76	1149*	1196
2.775	0.159	↓	1.13	1179*	1700
2.783	0.280		1.59	1202*	2200
2.791	0.422		1.99	1218*	2543
2.800	0.561		2.33	1234*	2778
2.807	0.69		2.59	1243*	2926
2.816	0.79		2.78	1257*	3028
2.825	0.90		2.97	1269*	3120
2.833	0.99		3.12	1280	3186
2.842	1.08		3.26	1291	3247
2.849	1.15		3.38	1300	3295
2.857	1.24		3.51	1306	3340
2.867	1.34		3.65	1315	3389
2.874	1.42		3.76	1320	3422
2.883	1.53		3.91	1326	3464
2.892	1.64		4.05	1332	3501
2.900	1.74		4.17	1337	3531
2.907	1.87		4.33	1341	3565
2.918	2.01		4.50	1350	3606
2.925	2.15		4.64	1354	3633
2.934	2.31		4.82	1360	3666
2.942	2.47		4.99	1364	3693
2.951	2.67		5.19	1368	3723
2.959	2.81		5.32	1372	3742
2.967	3.01		5.51	1380	3772
2.977	3.21		5.70	1385	3797
2.985	3.37		5.84	1388	3814
2.994	3.57		6.01	1389	3828
3.001	3.73		6.14	1389	3838
3.010	3.89		6.28	1388	3846
3.018	4.02		6.38	1384	3848
3.043	4.38	↓	6.67	1373	3849
3.068	4.66	0.076	6.87	1365	3849

*Extrapolated to wall temperature

TABLE IV (Concluded)

Forebody Velocities

M_∞ = 8.09

T_w/T_{o_∞} = 0.80 p_{o_∞} = 802 psia

Re_∞ = 3.3 x 10^6/ft T_{o_∞} = 1326°R

R, in.	p_o', psia	p_w, psia	M	T_o, °R	u, ft/sec
3.094	4.87	0.076	7.03	1356	3846
3.118	4.99	↓	7.12	1345	3834
3.143	5.13		7.22	1340	3832
3.169	5.24		7.29	1336	3829
3.195	5.32		7.35	1333	3828
3.218	5.39		7.39	1331	3827
3.245	5.44		7.43	1330	3827
3.269	5.46		7.45	1329	3826
3.319	5.51		7.48	1328	3826
3.370	5.54		7.50	1327	3826
3.422	5.55		7.51	1326	3825
3.522	5.57		7.53	1326	3826
3.772	5.57	0.076	7.53	1326	3826

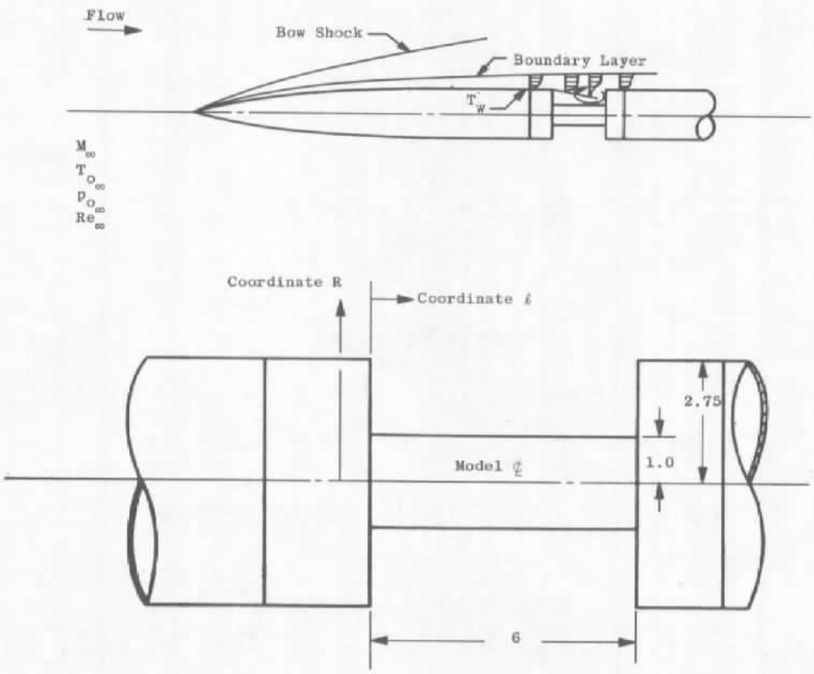

All Dimensions in Inches

Nomenclature for Cavity Flow Field Survey Data of Table V

TABLE V
CAVITY FLOW FIELD SURVEY DATA

M_∞ = 3.99 $\quad$ p_{o_∞} = 37 psia

T_W/T_{o_∞} = 0.75 $\quad$ T_{o_∞} = 675°R

Re_∞ = 2.4 x 10^6/ft $\quad$ ℓ = 0.8 in.

R, in.	p_o', psia	p, psia	M	T_o, °R	u, ft/sec
2.510	0.264	0.248	0.30	580	351
2.608	0.272	↓	0.37	580	431
2.657	0.277		0.40	581	465
2.707	0.307		0.56	584	643
2.756	0.432		0.93	593	1025
2.805	0.74		1.38	614	1426
2.854	1.53		2.10	637	1893
2.904	2.41		2.68	653	2150
2.953	4.19		3.57	661	2388
3.002	4.92		3.88	667	2452
3.051	4.67		3.75	669	2435
3.101	5.08		3.94	671	2469
3.120	5.15		3.97	671	2476
3.150	5.09		3.95	671	2466
3.150	5.15		3.97	671	2476
3.150	5.13		3.96	671	2472
3.199	5.03		3.92	671	2466
3.199	5.01		3.91	671	2460
3.248	5.02		3.92	670	2464
3.298	5.03	0.248	3.92	670	2464

TABLE V (Continued)

$M_\infty = 3.99$

$T_w/T_{o_\infty} = 0.75$

$\ell = 2.0$ in.

R, in.	p_o, psia	p, psia	M	T_o, °R	u, ft/sec
1.091	0.232	0.230	0.13	0	584
---	---		---	---	---
1.387	0.231		0.11	130	584
1.584	0.237		0.21	248	584
1.781	0.242		0.28	329	584
1.978	0.250		0.35	410	584
2.175	0.256		0.40	466	584
2.372	0.250		0.43	500	585
2.569	0.292		0.60	690	588
2.667	0.366		0.85	955	601
2.716	0.477		1.08	1180	614
2.766	0.69		1.39	1455	631
2.864	1.44		2.12	1936	661
2.913	2.04		2.56	2140	670
2.963	2.85		3.05	2300	677
3.012	3.37		3.32	2362	677
3.061	3.92		3.59	2420	678
3.110	4.40		3.81	2476	679
3.160	4.78		3.98	2486	
3.160	4.78		3.98	2486	
3.258	5.18		4.14	2510	
3.357	5.42		4.24	2520	
3.357	5.41		4.24	2520	
3.455	5.50		4.27	2520	
3.554	5.05		4.09	2502	
3.751	5.06		4.09	2502	
3.948	5.05	0.230	4.09	2502	679

TABLE V (Continued)

$M_\infty = 3.99$

$T_w/T_{o_\infty} = 0.75$

$\ell = 3.0$

R, in.	p_o', psia	p, psia	M	T_o, °R	u, ft/sec
1.795	0.228	0.227	0.10	118	582
1.992	0.236		0.24	282	582
2.189	0.243		0.32	375	582
2.288	0.249		0.37	432	582
2.383	0.260		0.53	610	583
2.485	0.289		0.60	688	586
2.583	0.360		0.84	942	598
2.682	0.544		1.20	1287	617
2.780	0.92		1.66	1654	641
2.879	1.66		2.30	2022	662
2.977	2.71		3.51	2394	671
3.076	3.81		3.56	2409	674
3.174	4.47		3.87	2466	675
3.273	4.79		4.00	2485	675
3.371	4.92		4.06	2492	674
3.470	5.02		4.10	2498	
3.568	5.13		4.15	2505	
3.667	5.29		4.21	2513	
3.765	5.42		4.27	2520	
3.864	5.01		4.10	2498	
3.962	4.99		4.09	2496	
4.061	5.01		4.10	2498	
4.159	5.01		4.10	2498	
4.258	5.03	0.227	4.11	2499	674

TABLE V (Continued)

$M_\infty = 3.99$

$T_w/T_{o_\infty} = 0.75$

$\ell = 4.0$ in.

R, in.	p_o', psia	p, psia	M	T_o, °R	u, ft/sec
1.968	0.242	0.235	0.22	259	584
2.165	0.255		0.34	398	584
2.263	0.265		0.42	489	585
2.362	0.285		0.54	624	589
2.460	0.328		0.71	808	594
2.559	0.410		0.93	1035	605
2.657	0.592		1.24	1328	624
2.756	0.95		1.65	1651	644
2.854	1.58		2.20	1981	664
2.904	1.97		2.48	2132	669
2.953	2.58		2.86	2243	675
3.002	3.10		3.15	2325	677
3.051	3.66		3.42	2389	678
3.150	4.41		3.77	2456	679
3.248	4.73		3.91	2479	
3.347	4.82		3.95	2485	
3.445	4.87		3.97	2488	
3.544	4.92		3.99	2491	
3.544	4.93		3.99	2491	
3.642	5.02		4.03	2497	
3.741	5.11		4.07	2503	
3.839	5.23		4.12	2510	
3.938	5.36		4.17	2517	
4.036	5.45		4.20	2520	
4.135	5.02		4.03	2497	
4.233	5.02		4.03	2497	
4.283	5.02		4.03	2497	
4.430	5.02		4.03	2497	
4.480	5.00	0.235	4.02	2496	679

TABLE V (Continued)

$M_\infty = 8.09$ $p_{o_\infty} = 800$ psia

$T_w/T_{o_\infty} = 0.4$ $T_{o_\infty} = 1345°R$

$Re_\infty = 3.3 \times 10^6/ft$ $\ell = 0.50$ in.

R, in.	p_o', psia	p, psia	M	T_o, °R	u, ft/sec
2.693	0.102	0.094	0.51	1098	808
2.693	0.100	0.093	0.45	1098	716
2.717	0.165	0.093	0.98	1106	1463
2.743	0.314	0.093	1.52	1122	2064
2.767	0.55	0.092	2.09	1143	2530
2.792	0.80	0.092	2.54	1175	2820
2.817	1.08	0.090	3.00	1205	3050
2.842	1.42	0.090	3.45	1240	3238
2.866	1.87	0.090	3.98	1278	3415
2.892	2.45	0.088	4.62	1325	3591
2.892	2.45	0.090	4.55	1325	3580
2.916	3.25	0.091	5.23	1364	3721
2.941	4.06	0.094	5.76	1394	3815
2.966	4.72	0.097	6.13	1415	3872
2.991	5.07	0.102	6.18	1408	3867
3.016	5.18	0.100	6.33	1388	3849
3.040	5.20	0.096	6.48	1372	3837
3.065	5.23	0.090	6.71	1357	3829
3.090	5.26	0.087	6.84	1349	3825
3.115	5.29	0.084	6.96	1347	3829
3.165	5.32	0.082	7.09	1345	3833
3.265	5.33	0.081	7.15	↓	3835
3.465	5.42	0.081	7.20	↓	3838
3.665	5.45	0.080	7.26	1345	3840

TABLE V (Continued)

M_∞ = 8.09

T_w/T_{o_∞} = 0.40

ℓ = 1.0 in.

R, in.	p_o', psia	p, psia	M	T_o, °R	u, ft/sec
2.692	0.114	0.089	0.64	1103	1002
2.742	0.198	0.089	1.14	1130	1673
2.766	0.297	0.090	1.48	1150	2051
2.792	0.430	0.089	1.84	1180	2392
2.816	0.593	0.088	2.21	1200	2669
2.841	0.79	0.087	2.58	1235	2910
2.866	1.06	0.087	3.01	1269	3134
2.866 (R)	1.06	0.087	3.01	1269	3134
2.892	1.39	0.087	3.48	1300	3324
2.892 (R)	1.39	0.083	3.55	1300	3344
2.916	1.82	0.084	4.06	1335	3507
2.940	2.34	0.083	4.63	1376	3660
2.965	3.06	0.085	5.27	1401	3776
2.992	3.91	0.086	5.89	1409	3846
3.015	4.73	0.090	6.37	1405	3876
3.040	5.41	0.094	6.66	1385	3866
3.065	5.78	0.091	6.99	1368	3861
3.090	5.91	0.099	6.80	1355	3832
3.115	5.83	0.097	6.79	1344	3816
3.165	5.50	0.090	6.85	1336	3808
3.266	5.37	0.076	7.37	1335	3832
3.464	5.39	0.078	7.28	1334	3826
3.664	5.43	0.077	7.36	1334	3830
5.863	5.45	0.078	7.36	1334	3830

TABLE V (Continued)

$M_\infty = 8.09$

$T_w/T_{o_\infty} = 0.40$

$\ell = 1.5$ in.

R, in.	p_o', psia	p, psia	M	T_o, °R	u, ft/sec
2.394	0.088	0.086	0.19	1070	304
2.593	0.097	↓	0.42	1088	667
2.692	0.151		0.96	1119	1446
2.741	0.272		1.43	1140	1993
2.766	0.373		1.73	1169	2293
2.791	0.502		2.05	1191	2556
2.816	0.669		2.39	1216	2791
2.841	0.88		2.74	1231	2979
2.866	1.16		3.19	1273	3202
2.891	1.52		3.65	1302	3372
2.941	2.47		4.68	1380	3674
2.991	3.85		5.87	1427	3868
3.015	4.53		6.37	1429	3909
3.040	5.11		6.77	1427	3931
3.091	5.93		7.29	1394	3912
3.139	6.16		7.43	1376	3893
3.165	6.04		7.36	1370	3881
3.190	5.82		7.23	1366	3870
3.215	5.63		7.11	1363	3860
3.239	5.51		7.03	1361	3853
3.265	5.45		6.99	1358	3846
3.290	5.42		6.97	1357	3844
3.340	5.38		6.95	1357	3843
3.440	5.36		6.93	1356	3841
3.538	5.39		6.95	1355	3840
3.738	5.41		6.96	1354	3839
3.938	5.44	0.086	6.98	1353	3839

TABLE V (Continued)

$M_\infty = 8.09$

$T_w/T_{o_\infty} = 0.40$

$\ell = 2.0$ in.

R, in.	p_o', psia	p, psia	M	T_o, °R	u, ft/sec
2.595	0.091	0.085	0.52	1085	818
2.645	0.129	↓	0.81	1100	1238
2.693	0.165		1.09	1120	1607
2.720	0.214		1.29	1135	1845
2.745	0.285		1.51	1151	2081
2.770	0.375		1.77	1169	2326
2.793	0.479		2.03	1186	2537
2.819	0.63		2.36	1210	2767
2.843	0.81		2.64	1228	2930
2.893	1.31		3.40	1280	3276
2.942	2.08		4.32	1339	3561
2.993	3.19		5.37	1390	3772
3.041	4.47		6.37	1403	3873
3.093	5.41		7.01	1387	3888
3.142	5.97		7.36	1362	3870
3.166	6.15		7.48	1352	3861
3.194	6.28		7.56	1347	3857
3.219	6.30		7.57	1344	3853
3.240	6.27		7.55	1342	3849
3.266	6.15		7.48	1340	3843
3.292	5.89		7.32	1338	3834
3.316	5.71		7.21	1336	3826
3.341	5.55		7.10	1335	3819
3.365	5.47	↓	7.05	1334	3815
3.365	5.47	0.085	7.05	1334	3815

TABLE V (Continued)

$M_\infty = 8.09$

$T_w/T_{o_\infty} = 0.40$

$\ell = 2.0$ in.

R, in.	p_o', psia	p, psia	M	T_o, °R	u, ft/sec
3.390	5.43	0.085	7.03	1334	3814
3.416	5.40	↓	7.01	↓	3813
3.440	5.39		7.00		3813
3.490	5.37		6.99		3812
3.540	5.38		7.00		3813
3.590	5.40		7.02		3814
3.690	5.40		7.02		3814
3.792	5.43	0.085	7.03	1334	3814

TABLE V (Continued)

$M_\infty = 8.09$

$T_W/T_{O_\infty} = 0.40$

$\ell = 3.0$ in.

R, in.	p_O', psia	p, psia	M	T_O, °R	u, ft/sec
2.196	0.076	0.074	0.42	1041	655
2.295	0.081	0.075	0.46	1048	718
2.395	0.082	0.076	0.49	1060	765
2.495	0.090	0.076	0.59	1075	917
2.595	0.135	0.075	0.99	1096	1469
2.642	0.185	0.073	1.26	1114	1796
2.691	0.259	0.073	1.56	1135	2112
2.743	0.379	0.073	1.93	1164	2443
2.791	0.552	0.072	2.37	1193	2753
2.841	0.83	0.072	2.92	1235	3058
2.890	1.22	0.072	3.58	1279	3324
2.940	1.81	0.073	4.35	1330	3554
2.991	2.67	0.074	5.25	1375	3739
3.040	3.63	0.078	6.00	1400	3843
3.090	4.49	0.080	6.56	1401	3883
3.141	5.14	0.090	6.62	1382	3860
3.189	5.67	0.095	6.79	1363	3843
3.240	6.16	0.102	6.84	1349	3826
3.290	6.41	0.105	6.87	1340	3815
3.315	6.49	0.106	6.86	1340	3814
3.339	6.56	0.109	6.81	1340	3811
3.366	6.61	0.111	6.79	1340	3810
3.391	6.60	0.112	6.75	1340	3808
3.415	6.53	0.111	6.72	1340	3806
3.439	6.35	0.111	6.64	1340	3803
3.489	5.86	0.105	6.56	1339	3796
3.598	5.44	0.093	6.72	1337	3802
3.689	5.40	0.087	6.90	1336	3811
3.788	5.44	0.085	7.01	1336	3816
3.988	5.48	0.087	6.97	1335	3813

TABLE V (Continued)

$M_\infty = 8.09$

$T_w/T_{o_\infty} = 0.40$

$\ell = 3.5$

R, in.	p_o', psia	p, psia	M	T_o, °R	u, ft/sec
2.494	0.099	0.069	0.81	1079	1226
2.593	0.164	0.071	1.20	1104	1722
2.643	0.220	0.070	1.47	1119	2014
2.692	0.306	0.070	1.76	1140	2289
2.742	0.435	0.070	2.14	1165	2586
2.792	0.62	0.070	2.57	1195	2858
2.841	0.89	0.069	3.10	1229	3116
2.891	1.22	0.070	3.71	1270	3345
2.891	1.28	0.069	3.73	1270	3350
2.941	1.81	0.069	4.47	1316	3556
2.991	2.51	0.070	5.23	1360	3716
3.041	3.25	0.074	5.81	1393	3817
3.190	5.38	0.093	6.67	1375	3852
3.240	5.90	0.095	6.91	1358	3842
3.289	6.23	0.102	6.85	1346	3822
3.289	6.23	0.101	6.90	1346	3825
3.339	6.42	0.105	6.87	1340	3815
3.363	6.51	0.107	6.84	1339	3812
3.389	6.57	0.109	6.82	1338	3809
3.413	6.63	0.109	6.84	1338	3811
3.440	6.67	0.110	6.85	1337	3809
3.463	6.68	0.111	6.82	1337	3808
3.489	6.64	0.110	6.81	1337	3807
3.513	6.53	0.111	6.73	1336	3801
3.563	6.06	0.109	6.55	1336	3791
3.614	5.63	0.101	6.57	1335	3790
3.663	5.46	0.090	6.84	1334	3804
3.713	5.39	0.088	6.89	1333	3806
3.813	5.43	0.087	6.95	1332	3807
3.913	5.44	0.086	7.00	1331	3809
4.114	5.50	0.085	7.07	1330	3811

TABLE V (Continued)

$M_\infty = 8.09$

$T_w/T_{o_\infty} = 0.40$

$\ell = 4.0$ in.

R, in.	p_o', psia	p, psia	M	T_o, °R	u, ft/sec
2.395	0.086	0.070	0.64	1054	979
2.494	0.121	0.071	0.95	1073	1404
2.593	0.193	0.070	1.35	1089	1869
2.644	0.262	0.069	1.61	1123	2146
2.693	0.358	0.069	1.93	1145	2423
2.743	0.495	0.068	2.32	1172	2701
2.793	0.69	0.067	2.78	1202	2961
2.843	0.96	0.067	3.27	1234	3178
2.892	1.31	0.067	3.86	1273	3384
2.941	1.75	0.068	4.42	1315	3546
2.991	2.31	0.068	5.12	1355	3697
3.041	2.98	0.069	5.78	1386	3805
3.091	3.74	0.073	6.29	1395	3857
3.141	4.45	0.078	6.62	1380	3857
3.189	5.05	0.085	6.76	1373	3855
3.189	5.00	0.087	6.65	1373	3849
3.240	5.54	0.091	6.84	1355	3834
3.290	5.94	0.096	6.89	1343	3820
3.339	6.24	---	---	1339	---
3.389	6.46	0.106	6.86	1338	3811
3.439	6.58	0.108	6.86	↓	↓
3.465	6.64	0.109	6.85	↓	↓
3.490	6.68	0.110	6.85	↓	3811
3.515	6.71	0.108	6.92	1338	3814
3.540	6.73	0.111	6.85	1339	3812
3.565	6.71	0.111	6.83	1339	3811
3.589	6.59	0.111	6.77	1340	3809
3.615	6.40	0.109	6.72	1339	3805
3.665	5.91	0.102	6.68	1338	3802
3.715	5.59	0.094	6.76	1336	3803
3.814	5.45	0.087	6.96	1335	3812
3.914	5.48	0.086	7.02	↓	3815
4.114	5.53	0.082	7.19	↓	3824
4.314	5.56	0.084	7.17	1335	3823

TABLE V (Continued)

$M_\infty = 8.09$

$T_w/T_{o_\infty} = 0.40$

$\ell = 4.75$ in.

R, in.	p_o', psia	p, psia	M	T_o, °R	u, ft/sec
2.295	0.073	0.067	0.48	1060	750
2.394	0.091	0.067	0.74	1073	1130
2.495	0.133	0.067	1.08	1094	1579
2.545	0.172	0.065	1.30	1109	1838
2.595	0.224	0.065	1.54	1125	2089
2.643	0.299	0.063	1.83	1142	2350
2.692	0.397	0.064	2.12	1164	2577
2.744	0.535	0.064	2.49	1188	2815
2.792	0.70	0.063	2.87	1214	3017
2.842	0.92	0.063	3.32	1245	3213
2.891	1.27	0.062	3.86	1282	3402
2.943	1.58	0.062	4.41	1317	3553
2.994	2.06	0.062	5.06	1358	3701
3.041	2.60	0.063	5.62	1384	3796
3.094	3.24	0.068	6.07	---	---
3.140	3.82	0.070	6.50	---	---
3.190	4.39	0.075	6.74	1374	3863
3.240	4.92	0.079	6.92	1361	3854
3.240	4.87	0.082	6.79	1361	3847
3.291	5.31	0.085	6.95	1352	3843
3.340	5.70	0.090	6.98	1344	3833
3.389	6.01	0.096	6.96	1340	3826
3.439	6.25	0.100	6.95	1338	3823
3.490	6.44	0.103	6.26	1338	3823
3.516	6.51	0.104	6.94	1338	3820
3.541	6.57	0.106	6.91	↓	3810
3.566	6.62	0.107	6.91	↓	3810
3.595	6.67	0.108	6.89	↓	3808
3.617	6.71	0.108	6.92	↓	3813
3.639	6.73	0.109	6.90	↓	3810
3.664	6.73	0.110	6.88	1338	3806
3.688	6.67	0.110	6.84	1339	3800
3.714	6.55	0.110	6.78	1339	3803
3.764	6.12	0.107	6.65	1340	3800
3.815	---	---	---	1338	---
3.913	5.49	0.087	6.96	1335	3810
4.014	5.50	0.086	7.04	1335	3811

TABLE V (Continued)

Reverse-Flow Survey

$M_\infty = 8.09$

$T_w/T_{o_\infty} = 0.40$

$\ell = 3.5$ in.

R, in.	p_o', psia	p, psia	M	T_o, °R	u, ft/sec
1.016	0.084	0.073	0.45	708*	575
1.040	0.092	0.073	0.57	776*	740
1.056	0.103	0.073	0.72	856*	983
1.070	0.119	0.073	0.87	935*	1213
1.104	0.124	0.072	0.92	965	1274
1.137	0.126	0.072	0.93	967	1309
1.161	0.124	0.071	0.92	979	1305
1.234	0.111	0.069	0.85	985	1222
1.334	0.095	0.069	0.69	985	1014
1.382	0.089	0.068	0.62	985	919
1.578	0.077	0.068	0.41	983	620
1.775	0.070	0.067	0.26	988	398
1.874	0.069	0.068	0.08	996	124

*Extrapolated to wall temperature

TABLE V (Continued)
Reverse-Flow Survey

$M_\infty = 8.09$

$T_w/T_{o_\infty} = 0.40$

$\ell = 4.0$ in.

R, in.	p_o', psia	p, psia	M	T_o, °R	u, ft/sec
1.016	0.091	0.070	0.62	781*	817
1.023	0.092	0.073	0.59	766*	774
1.033	0.099	0.073	0.68	811*	909
1.040	0.106	0.073	0.76	850*	1027
1.056	0.122	0.071	0.91	926*	1258
1.071	0.142	0.073	1.03	986*	1440
1.088	0.148	0.072	1.07	1006*	1500
1.120	0.149	0.071	1.08	997	1505
1.144	0.143	0.070	1.06	1009	1491
1.194	0.129	0.070	0.98	1009	1389
1.244	0.114	0.068	0.90	1002	1295
1.343	0.096	0.068	0.72	989	1056
1.537	0.082	0.068	0.52	985	779
1.733	0.072	0.068	0.29	996	445
1.832	0.070	0.068	0.18	1002	278

*Extrapolated to wall temperature

TABLE V (Continued)

Reverse-Flow Survey

$M_\infty = 8.09$

$T_w/T_{o_\infty} = 0.40$

$\ell = 4.5$ in.

R, in.	p_o', psia	p, psia	M	T_o, °R	u, ft/sec
1.016	0.105	0.074	0.72	816*	959
1.024	0.104	0.074	0.71	818*	950
1.030	0.110	0.073	0.79	848*	1063
1.040	0.116	0.074	0.83	868*	1122
1.048	0.140	0.074	1.00	949*	1376
1.056	0.153	0.074	1.07	980*	1482
1.072	0.169	0.074	1.16	1024*	1615
1.089	0.176	0.073	1.20	1040*	1671
1.112	0.173	0.072	1.20	1040	1671
1.138	0.164	0.071	1.17	1042	1640
1.161	0.156	0.071	1.13	1037	1592
1.210	0.136	0.069	1.03	1021	1465
1.308	0.109	0.067	0.86	1004	1246
1.406	0.095	0.068	0.70	996	1033
1.553	0.082	0.069	0.51	992	768
1.652	0.077	0.069	0.39	995	594
1.850	0.068	0.068	0.08	1018	125

*Extrapolated to wall temperature

TABLE V (Continued)

Reverse-Flow Survey

$M_\infty = 8.09$

$T_w/T_{o\infty} = 0.40$

$\ell = 4.75$ in.

R, in.	p_o', psia	p, psia	M	T_o, °R	u, ft/sec
1.016	0.119	0.075	0.84	884*	1146
1.025	0.125	0.076	0.87	898*	1190
1.031	0.147	0.076	1.00	961*	1385
1.041	0.163	0.076	1.11	1014*	1550
1.048	0.172	0.076	1.14	1030*	1597
1.056	0.180	0.076	1.19	1056*	1672
1.065	0.185	0.076	1.21	1056*	1693
1.072	0.187	0.075	1.23	1056*	1716
1.097	0.183	0.073	1.24	1056*	1729
1.121	0.175	0.072	1.20	1056	1683
1.170	0.158	0.071	1.14	1057	1616
1.219	0.141	0.069	1.06	1048	1522
1.317	0.116	0.066	0.93	1037	1353
1.416	0.100	0.068	0.77	1028	1143
1.611	0.082	0.068	0.51	1023	780
1.808	0.075	0.069	0.33	1033	515

*Extrapolated to wall temperature

TABLE V (Continued)

$M_\infty = 8.09$

$T_w/T_{o_\infty} = 0.80$

$\ell = 1.0$ in.

R, in.	p_o', psia	p, psia	M	T_o, °R	u, ft/sec
2.008	0.086	0.079	0.470	---	---
2.105	0.085	0.078	0.44	---	---
2.222	0.084	0.078	0.40	1142	653
2.308	0.080	0.078	0.340	1147	559
2.408	0.081	0.079	0.32	1154	528
2.505	0.080	0.081	0.32	1162	530
2.610	0.081	0.083	0.34	1170	564
2.708	0.110	0.085	0.71	1200	1151
2.733	0.171	0.085	1.07	1223	1656
2.758	0.306	0.086	1.55	1255	2218
2.783	0.52	0.086	2.07	1280	2666
2.808	0.76	0.083	2.59	1300	2997
2.835	1.05	0.085	3.04	1316	3208
2.859	1.37	0.085	3.48	1329	3367
2.885	1.66	0.086	3.82	1344	3474
2.908	2.04	0.087	4.22	1358	3575
2.933	2.44	0.089	4.58	1375	3659
2.958	3.00	0.091	5.02	1386	3734
2.980	3.52	0.093	5.38	1393	3784
2.991	4.12	0.094	5.81	1395	3827
3.035	4.61	0.097	6.04	1385	3831
3.060	4.95	0.100	6.18	1374	3828
3.088	5.12	0.101	6.26	1362	3817
3.115	5.20	0.102	6.26	1352	3803
3.138	5.25	0.097	6.46	1345	3805
3.165	5.31	0.098	6.47	1339	3797
3.189	5.36	0.096	6.56	1335	3797
3.215	5.41	0.091	6.76	1334	3807
3.243	5.46	0.092	6.75	1333	3805
3.268	5.51	0.092	6.79	1331	3805
3.293	5.53	0.088	6.94	1330	3811
3.318	5.55	0.091	6.87	1330	3807
3.345	5.56	0.092	6.83	1330	3805

TABLE V (Continued)

$M_\infty = 8.09$

$T_w/T_{o_\infty} = 0.80$

$\ell = 1.0$ in.

R, in.	p_o', psia	p, psia	M	T_o, °R	u, ft/sec
3.370	5.57	0.091	6.88	1330	3808
3.395	5.58	0.091	6.87	↓	3807
3.418	5.59	0.090	6.93	↓	3811
3.442	5.60	0.091	6.89	↓	3809
3.475	5.61	0.087	7.03	1330	3816
3.569	5.60	0.090	6.93	1329	3809
3.670	5.61	0.090	6.95	↓	3810
3.772	5.61	0.089	6.96	↓	3811
3.870	5.60	0.088	6.99	1329	3812

TABLE V (Continued)

M_∞ = 8.09 p_{o_∞} = 800 psia

T_w/T_{o_∞} = 0.80 T_{o_∞} = 1345°R

Re_∞ = 3.3 x 10^6/ft ℓ = 0.10 in.

R, in.	p_o', psia (ℓ = 0.10)	p, psia (ℓ = 0.10)	M	T_o, °R (ℓ = 0.20)	u, ft/sec
2.767	0.105	0.090	0.54	1215	897
2.771	0.135	0.090	0.81	1230	1309
2.785	0.197	0.089	1.14	1250	1760
2.793	0.279	0.090	1.41	1265	2079
2.801	0.402	0.090	1.76	1278	2423
2.810	0.529	0.089	2.06	1285	2662
2.817	0.65	0.087	2.33	1295	2845
2.826	0.80	0.089	2.57	1305	2987
2.834	0.89	0.088	2.73	1312	3071
2.842	1.00	0.088	2.91	1322	3159
2.867	1.30	0.086	3.36	1333	3331
2.893	1.62	0.089	3.71	1345	3442
2.917	1.99	0.091	4.08	1360	3544
2.944	2.42	0.091	4.50	1375	3639
2.967	2.89	0.092	4.90	1386	3712
2.994	3.41	0.089	5.42	1392	3779
3.020	3.87	0.089	5.77	1389	3809
3.045	4.26	0.088	6.10	1384	3829
3.070	4.52	0.087	6.33	1379	3836
3.119	4.95	0.086	6.64	1364	3837
3.169	5.19	0.089	6.71	1350	3820
3.219	5.37	0.089	6.83	1343	3817
3.269	5.46	0.090	6.85	1339	3812

TABLE V (Continued)

$M_\infty = 8.09$

$T_w/T_{o_\infty} = 0.80$

$\ell = 0.10$ in.

R, in.	p_o', psia (ℓ = 2.0 in.)	p, psia	M	T_o, °R (ℓ = 0.20 in.)	u, ft/sec
3.320	5.51	0.089	6.89	1337	3811
3.372	5.55	0.090	6.88	↓	↓
3.420	5.57	0.090	6.89	↓	↓
3.420	5.57	0.091	6.88	1337	↓
3.470	5.58	0.090	6.90	1336	3811
3.521	5.58	0.088	6.99	↓	3815
3.570	5.58	0.090	6.91	↓	3811
3.570	5.57	0.090	6.92	↓	3812
3.621	5.58	0.090	6.92	↓	3812
3.672	5.59	0.090	6.94	↓	3813
3.772	5.58	0.090	6.93	↓	3812
3.874	5.58	0.087	7.03	↓	3817
3.994	5.60	0.089	6.96	↓	3814
4.099	5.62	0.088	7.03	↓	3817
4.196	5.64	0.089	6.98	↓	3815
4.299	5.66	0.088	7.03	↓	3817
4.399	5.68	0.089	7.02	↓	3817
4.501	5.69	0.088	7.07	↓	3819
4.600	5.71	0.089	7.03	↓	3817
4.785	5.77	0.089	7.06	1336	3819

TABLE V (Continued)

$M_\infty = 8.09$

$T_w/T_{o_\infty} = 0.80$

$\ell = 2.0$ in.

R, in.	p_o', psia ($\ell = 2.0$ in.)	p, psia ($\ell = 2.0$ in.)	M	T_o, °R ($\ell = 2.125$ in.)	u, ft/sec
2.007	0.088	0.080	0.36	1130	586
2.110	0.084	0.074	0.44	1134	713
2.207	0.085	0.074	0.45	1139	730
2.307	0.086	0.076	0.43	1148	701
2.410	0.084	0.075	0.42	1157	688
2.458	0.085	0.076	0.42	1161	689
2.509	0.083	0.075	0.44	1166	722
2.559	0.085	0.077	0.47	1173	772
2.610	0.094	0.079	0.59	1184	962
2.636	0.108	0.081	0.69	1189	1114
2.657	0.123	0.082	0.82	1196	1305
2.683	0.153	0.081	1.01	1212	1571
2.710	0.199	0.083	1.22	1223	1836
2.736	0.282	0.083	1.49	1240	2140
2.761	0.375	0.083	1.77	1253	2408
2.787	0.526	0.083	2.13	1272	2696
2.810	0.68	0.083	2.45	1283	2899
2.833	0.88	0.083	2.79	1293	3075
2.859	1.10	0.083	3.16	1307	3234
2.884	1.36	0.084	3.50	1324	3361
2.910	1.66	0.084	3.87	1336	3468
2.934	1.99	0.084	4.25	1349	3562
2.959	2.38	0.086	4.58	1366	3640
2.985	2.80	0.088	4.94	1379	3707
3.010	3.26	0.088	5.33	1387	3764
3.037	3.77	0.090	5.66	1394	3805
3.060	4.19	0.092	5.91	1396	3829
3.086	4.63	0.094	6.14	1394	3845
3.112	5.05	0.095	6.40	1389	3856
3.136	5.63	0.101	6.37	1384	3847
3.162	5.64	0.103	6.51	1375	3843
3.187	5.86	0.105	6.56	1364	3831
3.214	6.01	0.106	6.60	1357	3824

TABLE V (Continued)

$M_\infty = 8.09$

$T_w/T_{o_\infty} = 0.80$

$\ell = 2.0$ in.

R, in.	p_o', psia (ℓ=2.0 in.)	p, psia	M	T_o, °R (ℓ = 2.125 in.)	u, ft/sec
3.236	6.06	0.108	6.57	1352	3815
3.264	6.04	0.108	6.56	1345	3804
3.287	5.96	0.107	6.54	1342	3799
3.313	5.85	0.104	6.58	1338	3795
3.339	5.76	0.102	6.59	1336	3792
3.363	5.70	0.096	6.77	1335	3802
3.387	5.67	0.096	6.73	1334	3799
3.411	5.65	0.095	6.78	↓	3801
3.437	5.64	0.093	6.82	↓	3803
3.483	5.63	0.091	6.90	↓	3808
3.580	5.62	0.092	6.88	↓	3807
3.681	5.63	0.090	6.93	↓	3809
3.764	5.63	0.089	6.97	↓	3811
3.866	5.63	0.090	6.95	↓	3810
3.967	5.64	0.090	6.97	↓	3811
4.168	5.67	0.089	6.99	1334	3812

TABLE V (Continued)

$M_\infty = 8.09$

$T_w/T_{o_\infty} = 0.80$

$\ell = 3.0$ in.

R, in.	p_o', psia	p, psia	M	T_o, °R	u, ft/sec
2.158	0.071	0.071	0.43	1144	701
2.206	0.076	0.072	0.48	1144	779
2.260	0.078	0.073	0.49	1147	796
2.308	0.078	0.072	0.52	1151	844
2.360	0.081	0.073	0.52	1155	845
2.410	0.081	0.074	0.52	1161	847
2.460	0.082	0.073	0.56	1166	911
2.510	0.085	0.074	0.59	1171	959
2.535	0.091	0.075	0.65	1175	1051
2.560	0.099	0.075	0.73	1179	1170
2.582	0.108	0.074	0.81	1185	1287
2.608	0.121	0.074	0.92	1193	1443
2.632	0.145	0.072	1.09	1199	1666
2.660	0.179	0.072	1.24	1210	1852
2.682	0.216	0.071	1.42	1219	2055
2.708	0.272	0.068	1.65	1225	2282
2.732	0.337	0.070	1.83	1238	2447
2.759	0.421	0.069	2.08	1250	2644
2.783	0.53	0.070	2.33	1263	2815
2.810	0.65	0.070	2.62	1276	2983
2.835	0.79	0.071	2.88	1287	3111
2.860	0.98	0.071	3.23	1299	3254
2.885	1.16	0.072	3.49	1311	3347
2.908	1.39	0.073	3.81	1324	3445
2.935	1.65	0.074	4.13	1339	3533
2.958	1.93	0.073	4.48	1350	3609
2.985	2.25	0.075	4.79	1365	3675
3.012	2.64	0.075	5.21	1376	3742

TABLE V (Continued)

$M_\infty = 8.09$

$T_w/T_{o_\infty} = 0.80$

$\ell = 3.0$ in.

R, in.	p_o', psia	p, psia	M	T_o, °R	u, ft/sec
3.035	3.00	0.077	5.45	1385	3780
3.061	3.41	0.080	5.73	1392	3817
3.084	3.78	0.082	5.96	1396	3841
3.112	4.18	0.084	6.20	1393	3855
3.135	4.53	0.088	6.31	1389	3857
3.162	4.90	0.090	6.48	1385	3862
3.182	5.19	0.097	6.41	1379	3850
3.212	5.48	0.097	6.58	1367	3843
3.233	5.71	0.103	6.54	1362	3835
3.262	5.92	0.103	6.66	1351	3826
3.288	6.07	0.105	6.67	1347	3820
3.310	6.20	0.106	6.70	1342	3815
3.338	6.29	0.107	6.73	1339	3813
3.360	6.34	0.106	6.79	1337	3813
3.386	6.34	0.108	6.74	1336	3809
3.410	6.29	0.108	6.70	1335	3805
3.438	6.20	0.107	6.68	1334	3803
3.460	6.09	0.104	6.70	1333	3802
3.488	5.94	0.104	6.64	1333	3800
3.512	5.85	0.101	6.68	1333	3802
3.537	5.78	0.099	6.71	1333	3803
3.562	5.73	0.097	6.76	1333	3806
3.585	5.70	0.093	6.88	1333	3838
3.613	5.68	0.093	6.85	1333	3811
3.662	5.67	0.093	6.86	1333	3811
3.716	5.66	0.091	6.92	1333	3814
3.817	5.66	0.088	7.06	1333	3821
3.917	5.66	0.090	6.98	1333	3817

TABLE V (Continued)

M_∞ = 8.09

T_w/T_{o_∞} = 0.80

ℓ = 4.0 in.

R, in.	p_o', psia	p, psia	M	T_o, °R	u, ft/sec
2.308	0.067	0.064	0.41	1150	670
2.360	0.070	0.065	0.48	1155	781
2.416	0.078	0.065	0.59	1160	952
2.459	0.086	0.066	0.68	1165	1088
2.513	0.104	0.066	0.87	1173	1361
2.557	0.127	0.065	1.05	1186	1604
2.582	0.147	0.065	1.17	1191	1753
2.609	0.173	0.064	1.32	1198	1928
2.636	0.205	0.065	1.45	1204	2069
2.659	0.241	0.064	1.61	1216	2233
2.682	0.287	0.063	1.78	1221	2385
2.710	0.348	0.063	1.98	1230	2547
2.736	0.415	0.063	2.18	1240	2693
2.761	0.490	0.062	2.39	1250	2829
2.786	0.57	0.063	2.61	1263	2957
2.810	0.68	0.063	2.86	1268	3074
2.836	0.81	0.063	3.11	1278	3180
2.859	0.93	0.060	3.41	1290	3291
2.885	1.09	0.063	3.61	1301	3360
2.910	1.26	0.061	3.96	1312	3456
2.935	1.44	0.063	4.16	1323	3511
2.960	1.68	0.064	4.48	1335	3582
2.985	1.90	0.064	4.78	1348	3644
3.009	2.16	0.064	5.07	1360	3697
3.035	2.43	0.066	5.29	1373	3739
3.059	2.72	0.067	5.59	1380	3779
3.086	3.05	0.069	5.83	1389	3812
3.110	3.38	0.072	6.02	1390	3829

TABLE V (Continued)

$M_\infty = 8.09$

$T_w/T_{o_\infty} = 0.80$

$\ell = 4.0$ in.

R, in.	p_o', psia	p, psia	M	T_o, °R	u, ft/sec
3.134	3.71	0.075	6.19	1390	3841
3.160	4.09	0.074	6.50	1388	3860
3.186	4.43	0.079	6.56	1382	3856
3.212	4.76	0.082	6.68	1375	3853
3.237	5.08	0.085	6.77	1369	3850
3.262	5.30	0.094	6.58	1363	3830
3.288	5.54	0.097	6.65	1354	3822
3.313	5.76	0.099	6,69	1350	3819
3.337	5.93	0.099	6.78	1345	3815
3.362	6.07	0.103	6.74	1340	3807
3.388	6.18	0.104	6.76	1339	3807
3.414	6.27	0.105	6.78	1337	3805
3.438	6.34	0.104	6.86	1336	3807
3.462	6.40	0.107	6.80	1336	3805
3.489	6.45	0.108	6.78	1335	3802
3.513	6.47	0.107	6.82	↓	3804
3.539	6.47	0.109	6.76	↓	3801
3.562	6.42	0.108	6.78	↓	3802
3.588	6.33	0.109	6.70	↓	3798
3.614	6.17	0.107	6.68	↓	3797
3.638	6.06	0.104	6.69	↓	3798
3.665	5.93	0.099	6.79	↓	3802
3.688	5.84	0.098	6.79	↓	3802
3.715	5.77	0.094	6.88	↓	3807
3.740	5.73	0.095	6.88	↓	3807
3.789	5.69	0.094	6.89	↓	3808
3.840	5.67	0.092	6.92	↓	3809
3.890	5.67	0.091	6.93	↓	3810
3.991	5.69	0.090	6.94	↓	3811
4.093	5.70	0.088	6.98	1335	3812

TABLE V (Continued)

M_∞ = 8.09

T_w/T_{o_∞} = 0.80

ℓ = 4.75 in.

R, in.	p_o', psia	p, psia	M	T_o, °R	u, ft/sec
2.305	0.064	0.063	0.38	1165	627
2.358	0.073	0.064	0.56	1172	911
2.409	0.083	0.064	0.70	1178	1124
2.460	0.097	0.065	0.84	1185	1327
2.509	0.123	0.065	1.03	1194	1584
2.556	0.159	0.065	1.23	1203	1832
2.580	0.184	0.063	1.38	1209	2001
2.609	0.213	0.062	1.53	1217	2159
2.630	0.250	0.063	1.64	1224	2267
2.655	0.296	0.065	1.78	1230	2394
2.685	0.349	0.064	1.96	1239	2543
2.708	0.400	0.063	2.14	1246	2675
2.734	0.467	0.062	2.32	1253	2793
2.760	0.545	0.063	2.51	1263	2908
2.785	0.63	0.062	2.73	1272	3024
2.810	0.73	0.062	2.95	1279	3123
2.835	0.83	0.061	3.19	1289	3222
2.861	0.96	0.062	3.42	1299	3306
2.885	1.09	0.061	3.67	1309	3386
2.910	1.24	0.061	3.91	1319	3455
2.935	1.41	0.061	4.18	1329	3523
2.962	1.60	0.060	4.51	1341	3595
2.985	1.82	0.062	4.75	1351	3644
3.010	2.04	0.062	5.03	1359	3692
3.037	2.28	0.063	5.28	1369	3734
3.062	2.56	0.063	5.59	1374	3771
3.085	2.80	0.062	5.90	1380	3807
3.112	3.12	0.065	6.06	1381	3820

TABLE V (Concluded)

$M_\infty = 8.09$

$T_w/T_{o_\infty} = 0.80$

$\ell = 4.75$ in.

R, in.	p_o', psia	p, psia	M	T_o, °R	u, ft/sec
3.137	3.36	0.067	6.21	1382	3834
3.162	3.64	0.069	6.39	1382	3846
3.183	3.92	0.071	6.51	1381	3851
3.212	4.20	0.074	6.61	1377	3853
3.240	4.52	0.077	6.73	1372	3852
3.262	4.76	0.080	6.77	1369	3850
3.288	5.00	0.080	6.94	1364	3852
3.315	5.24	0.087	6.79	1359	3837
3.337	5.43	0.088	6.91	1353	3835
3.362	5.63	0.092	6.86	1348	3825
3.388	5.80	0.095	6.86	1344	3820
3.414	5.96	0.096	6.93	1342	3821
3.438	6.08	0.099	6.88	1340	3815
3.462	6.19	0.101	6.87	1339	3813
3.488	6.28	0.102	6.88	1338	3812
3.515	6.34	0.105	6.83	1337	3808
3.540	6.40	0.105	6.86	1336	3808
3.562	6.43	0.107	6.82	1336	3806
3.590	6.45	0.107	6.82	1336	3806
3.615	6.47	0.107	6.84	1335	3806
3.640	6.48	0.108	6.81	1335	3804
3.663	6.48	0.108	6.79	1336	3805
3.690	6.43	0.108	6.76	1336	3803
3.715	6.33	0.105	6.81	1336	3806
3.740	6.20	0.106	6.71	1335	3799
3.768	6.05	0.105	6.66	1335	3796
3.795	5.95	0.090	7.14	1335	3821
3.819	5.86	0.099	6.74	1335	3800
3.843	5.80	0.098	6.76	1335	3806
3.868	5.76	0.101	6.64	1335	3796
3.892	5.73	0.093	6.91	1335	3810

APPENDIX I
RELATIONSHIP BETWEEN VELOCITY AND TOTAL TEMPERATURE PROFILES: CROCCO'S RELATION

In Ref. 8, p. 1045, it is pointed out that for the case of constant wall temperature, Prandtl number of one, and zero pressure gradient, the momentum equation (Eq. (26.5a) of Ref. 8) and the energy equation (Eq. (26.9) of Ref. 8) take on the same form if

$$T_o = au + b$$

where T_o is the local stagnation temperature and u is the velocity. Since the differential equations are the same, then either a solution of the momentum equation or an experiment yielding the velocity distribution automatically gives the distribution of T_o according to the relation

$$T_o = au + b$$

The constants a and b may be obtained from the boundary conditions that $T_o = T_w$ when $u = 0$, and $T_o = T_{o_\infty}$ when $u = u_\infty$; thus,

$$\frac{T_o - T_w}{T_{o_\infty} - T_w} = \frac{u}{u_\infty} \qquad \text{(Eq. (26.11), Ref. 8)}$$

All of the above assume a Prandtl number of one, which is close for air with its Prandtl number ~ 0.7.

The variation of T_o with distance through the boundary layer for air with its Prandtl number less than one is illustrated in Ref. 8 on p. 1035, and a representative experiment for the insulated wall case is shown in Fig. 27.11b on p. 1115. The rise of T_o above both the wall temperature and the free-stream stagnation temperature is required for conservation of energy in the boundary-layer flow.

Since it is the form of the differential equations for momentum and energy which yields the Crocco relation $\frac{T_o - T_w}{T_{o_\infty} - T_w} = \frac{u}{u_\infty}$, and the boundary conditions determine the constants a and b, any solution of these differential equations for the velocity profile, such as the solution for the profile in a mixing layer, will give a corresponding total temperature distribution. In a mixing layer between a stream at velocity u_∞ and total temperature T_{o_∞} and a still air region at $u = 0$, $T_o = T_{o_{u=0}}$, the result follows that

$$\frac{T_o - T_{o_{u=0}}}{T_{o_\infty} - T_{o_{u=0}}} = \frac{u}{u_\infty}$$

This relation is Crocco's relation for a mixing layer as described above, and it is one of the assumptions made by Korst and Chow (Ref. 5) in their theoretical development.

APPENDIX II
UNIVERSAL VELOCITY PROFILE

The turbulent shearing stress for a two-dimensional parallel flow is (Ref. 12, Eq. (19.4))

$$\tau = -\rho \overline{u'v'} \tag{II-1}$$

This expression contains the turbulent velocity fluctuation terms u' and v'. These quantities may be related to the mean velocity, $\bar{u}$, through Prandtl's mixing length concept (Ref. 12, p. 477) leading to the expression of turbulent shearing stress as

$$\tau = \rho \ell^2 \left| \frac{\partial \bar{u}}{\partial y} \right| \frac{\partial \bar{u}}{\partial y} \quad \text{(Eq. (19.6), Ref. 12)}$$

or, for $\frac{\partial \bar{u}}{\partial y} > 0$, as

$$\tau = \rho \ell^2 \left(\frac{\partial \bar{u}}{\partial y} \right)^2 \tag{II-2}$$

If a generally valid assumption may be made about the variation of turbulent shearing stress with y through a boundary layer and an equally generally true assumption made about the variation with y of the mixing length ℓ with distance in the boundary layer, then Eq. (II-2) becomes an ordinary differential equation for the variation of $\bar{u}$ with y, giving as its solution the velocity profile. Prandtl assumed that:

1. The mixing length, ℓ, varies linearly with y, giving

$$\ell = Ky \quad \text{(Ref. 12, Eq. (19.26))}$$

2. The turbulent shearing stress is constant across the boundary layer and equal to the value at the wall

$$\tau = \tau_o = \tau_w$$

Introducing the "friction velocity" u_τ (u_{*_o} of Ref. 12)

$$u_\tau = \sqrt{\frac{\tau_w}{\rho}}$$

integration of Eq. (II-2) gives Eq. (19.27) of Ref. 12,

$$\bar{u} = \frac{u_\tau}{K} \ln y + C \tag{II-3}$$

where C is to be resolved from a match with the laminar sublayer. Experiment has yielded the constants K and C giving, for a smooth wall,

$$\frac{u}{u_\tau} = 5.5 + 5.75 \log\left(y \frac{u_\tau}{\eta_w}\right) \quad \text{(Ref. 12, Eq. (20.14))}$$

where ν is to be evaluated at the wall temperature for the compressible flow case (Ref. 12, p. 546).

The assumption that the velocity is linear with y in the laminar sublayer gives

$$\frac{u}{u_\tau} = y \frac{u_\tau}{\nu_w} \tag{II-4}$$

in this region, since

$$\frac{u}{y} = \frac{(u_\tau)^2}{\nu_w} = \frac{\tau_w \rho_w}{\rho_w \mu_w} = \frac{\mu_w \left(\frac{du}{dy}\right)_w}{\mu_w} = \left(\frac{du}{dy}\right)_w$$

Reference 12, Fig. 21.8, p. 546, shows the application of these concepts to another case in hypersonic boundary-layer flow.

APPENDIX III
ERROR FUNCTION PROFILE

Prandtl assumed that for a free turbulent shear layer, away from the restraining influence of a wall, (Fig. 11a) the virtual kinematic viscosity, ϵ, was constant across the shear layer and equal to the velocity difference across the layer times a length proportional to the width b of the layer (Ref. 12, p. 481). The resulting expression for shear stress is

$$\tau = \rho K_1 b (\bar{u}_{max} - \bar{u}_{min}) \frac{d\bar{u}}{dy} \quad \text{(Eq. (23.5) of Ref. 12)}$$

If it is further assumed that the shear, or mixing layer, grows in width b linearly with distance x, then Eq. (23. 1), Ref. 12, becomes

$$u \frac{\partial u}{\partial x} + v \frac{\partial u}{\partial y} = \epsilon \frac{\partial^2 u}{\partial y^2} \quad \text{(Eq. (23.25), Ref. 12)} \qquad \text{(III-1)}$$

with

$$\epsilon = K_1 \; cx \; (u_1 - u_2) \quad \text{(Eq. (23.26) Ref. 12)}$$

Equation (III-1) is a partial differential equation relating the velocities u and v to the space variables y and x. If the velocity profiles are assumed to be similar to each other and to vary linearly in width with increasing distance, then they may be reduced to one representative profile by dividing the y coordinate by the x coordinate. Thus the assumption of linear similarity allows all profiles in y and x to be reduced to one profile in the single variable, y/x. A scale factor, σ, is applied to account for the actual rate of growth in width of the mixing layer and is inversely related to the turbulent eddy kinematic viscosity, ϵ, through the relation

$$\sigma = \frac{1}{2\sqrt{K_1 C}} \; ; \; u_{min} = 0$$

or

$$\sigma = \frac{1}{2\sqrt{\frac{\epsilon}{x\,u_{max}}}} \; ; \; u_{min} = 0$$

The greater the turbulent eddy kinematic viscosity, the less the value of σ and the greater is the spreading rate of the velocity profiles.

If the continuity equation is accounted for by the introduction of a stream function, ψ, which contains both u and v velocities, then the partial differential equation, Eq. (1), is reduced to an ordinary differential equation in the velocity variable, ψ, and the space variable, $\sigma y/x$, becoming, after other definitions, (Ref. 12, p. 598),

$$F''' + 2\sigma^2 F F'' = 0 \quad \text{(Eq. (23.27), Ref. 12)} \qquad \text{(III-2)}$$

This equation was solved by Goertler, and the sum of the first two terms of the solution F_0 and F_1 gives the error function profile for free mixing layers,

$$\frac{u}{u_\delta} = \frac{1}{2}\left[1 + \text{erf}\left(\sigma \frac{y}{x}\right)\right] \qquad \text{(III-3)}$$

where U_1 and U_2 of Ref. 12 are taken to be U_δ and 0, respectively, to correspond to the present work.

The coefficient σ relates the mathematical assumptions of similarity of the velocity profiles and linear growth rate of the width of the mixing layer to the actual growth rate of an experimental mixing layer. This coefficient is not known a priori but must be determined by experiment. Also, the above theoretical development describes the mixing between two uniform streams. Thus the origin of the mixing layer occurs at the point where a uniform stream at u_δ has just contacted still fluid at $u = 0$. This corresponds to separation of the flow from a body with zero boundary-layer thickness (Fig. 11a). The assumption is made, for the case where a boundary layer is present initially, that the velocity profiles of the mixing layer assume the error function form within a few boundary-layer thicknesses of the separation point. A fictitious point of origin (Fig. 11b) for the linearly related mixing layer profiles may then be found by extrapolating upstream to the point of zero mixing layer thickness. This point must be located experimentally, together with the coefficient σ.

UNCLASSIFIED

Security Classification

DOCUMENT CONTROL DATA - R&D

(Security classification of title, body of abstract and indexing annotation must be entered when the overall report is classified)

1. ORIGINATING ACTIVITY (Corporate author) Arnold Engineering Development Center, ARO, Inc., Operating Contractor, Arnold Air Force Station, Tennessee	2a. REPORT SECURITY CLASSIFICATION UNCLASSIFIED 2b. GROUP N/A

3. REPORT TITLE

TURBULENT CAVITY FLOW INVESTIGATION AT MACH NUMBERS 4 AND 8

4. DESCRIPTIVE NOTES (Type of report and inclusive dates)

N/A

5. AUTHOR(S) (Last name, first name, initial)

Rhudy, J. P., and Magnan, J. D., Jr., ARO, Inc.

6. REPORT DATE	7a. TOTAL NO. OF PAGES	7b. NO. OF REFS
June 1966	76	12

8a. CONTRACT OR GRANT NO. AF40(600)-1200	9a. ORIGINATOR'S REPORT NUMBER(S) AEDC-TR-66-73
b. PROJECT NO. 8953	
c. Program Element 62405334	9b. OTHER REPORT NO(S) (Any other numbers that may be assigned this report)
d. Task 895303	N/A

10. AVAILABILITY/LIMITATION NOTICES

Qualified users may obtain copies of this report from DDC, and each transmittal to foreign governments or foreign nationals must have prior approval of AEDC.

11. SUPPLEMENTARY NOTES	12. SPONSORING MILITARY ACTIVITY
N/A	Arnold Engineering Development Center, Air Force Systems Command, Arnold Air Force Station, Tennessee

13. ABSTRACT An experimental investigation of turbulent flow over a cavity in an aerodynamic surface has been conducted. The test was carried out at nominal Mach numbers of 4 and 8, with Reynolds numbers based on free-stream conditions and length of body ahead of the cavity of 8.0×10^6 and 11.0×10^6, respectively. Two conditions of wall-to-free-stream stagnation temperature ratio, 0.4 and 0.8, were tested at $M_\infty = 8.09$, whereas at $M_\infty = 3.99$, the temperature ratio was 0.75. For all tests, the ratio of initial boundary-layer thickness to cavity depth was approximately 0.2. Measurements were made of surface pressure and temperature, and flow field surveys of pitot and static pressures and total temperature were performed. The test results showed that the recirculating fluid temperature was not less than 0.7 times the free-stream stagnation temperature despite decrease of the wall temperature to 0.4 the free-stream value. A satisfactory correlation was obtained between the experimental velocities and the error function profile of Goertler, and the distribution of total temperature across the mixing layer was adequately described by Crocco's linear relation of total temperature and velocity. A value of the mixing coefficient near 12 was found regardless of Mach number or wall-to-free-stream stagnation temperature ratio.

DD FORM 1 JAN 64 1473

UNCLASSIFIED

Security Classification

14 KEY WORDS	LINK A		LINK B		LINK C	
	ROLE	WT	ROLE	WT	ROLE	WT
airflow						
turbulence						
surface cavity						
supersonic flow						
hypersonic flow						
pressure measurements						
temperature measurements						

INSTRUCTIONS

1. ORIGINATING ACTIVITY: Enter the name and address of the contractor, subcontractor, grantee, Department of Defense activity or other organization *(corporate author)* issuing the report.

2*a*. REPORT SECURITY CLASSIFICATION: Enter the overall security classification of the report. Indicate whether "Restricted Data" is included. Marking is to be in accordance with appropriate security regulations.

2*b*. GROUP: Automatic downgrading is specified in DoD Directive 5200.10 and Armed Forces Industrial Manual. Enter the group number. Also, when applicable, show that optional markings have been used for Group 3 and Group 4 as authorized.

3. REPORT TITLE: Enter the complete report title in all capital letters. Titles in all cases should be unclassified. If a meaningful title cannot be selected without classification, show title classification in all capitals in parenthesis immediately following the title.

4. DESCRIPTIVE NOTES: If appropriate, enter the type of report, e.g., interim, progress, summary, annual, or final. Give the inclusive dates when a specific reporting period is covered.

5. AUTHOR(S): Enter the name(s) of author(s) as shown on or in the report. Enter last name, first name, middle initial. If military, show rank and branch of service. The name of the principal author is an absolute minimum requirement.

6. REPORT DATE: Enter the date of the report as day, month, year; or month, year. If more than one date appears on the report, use date of publication.

7*a*. TOTAL NUMBER OF PAGES: The total page count should follow normal pagination procedures, i.e., enter the number of pages containing information.

7*b*. NUMBER OF REFERENCES: Enter the total number of references cited in the report.

8*a*. CONTRACT OR GRANT NUMBER: If appropriate, enter the applicable number of the contract or grant under which the report was written.

8*b*, 8*c*, & 8*d*. PROJECT NUMBER: Enter the appropriate military department identification, such as project number, subproject number, system numbers, task number, etc.

9*a*. ORIGINATOR'S REPORT NUMBER(S): Enter the official report number by which the document will be identified and controlled by the originating activity. This number must be unique to this report.

9*b*. OTHER REPORT NUMBER(S): If the report has been assigned any other report numbers *(either by the originator or by the sponsor)*, also enter this number(s).

10. AVAILABILITY/LIMITATION NOTICES: Enter any limitations on further dissemination of the report, other than those imposed by security classification, using standard statements such as:

(1) "Qualified requesters may obtain copies of this report from DDC."

(2) "Foreign announcement and dissemination of this report by DDC is not authorized."

(3) "U. S. Government agencies may obtain copies of this report directly from DDC. Other qualified DDC users shall request through
_______________________________."

(4) "U. S. military agencies may obtain copies of this report directly from DDC. Other qualified users shall request through
_______________________________."

(5) "All distribution of this report is controlled. Qualified DDC users shall request through
_______________________________."

If the report has been furnished to the Office of Technical Services, Department of Commerce, for sale to the public, indicate this fact and enter the price, if known.

11. SUPPLEMENTARY NOTES: Use for additional explanatory notes.

12. SPONSORING MILITARY ACTIVITY: Enter the name of the departmental project office or laboratory sponsoring *(paying for)* the research and development. Include address.

13. ABSTRACT: Enter an abstract giving a brief and factual summary of the document indicative of the report, even though it may also appear elsewhere in the body of the technical report. If additional space is required, a continuation sheet shall be attached.

It is highly desirable that the abstract of classified reports be unclassified. Each paragraph of the abstract shall end with an indication of the military security classification of the information in the paragraph, represented as *(TS)*, *(S)*, *(C)*, or *(U)*.

There is no limitation on the length of the abstract. However, the suggested length is from 150 to 225 words.

14. KEY WORDS: Key words are technically meaningful terms or short phrases that characterize a report and may be used as index entries for cataloging the report. Key words must be selected so that no security classification is required. Identifiers, such as equipment model designation, trade name, military project code name, geographic location, may be used as key words but will be followed by an indication of technical context. The assignment of links, rules, and weights is optional.